CHAPTER 9 BUMPS

9.1 INTRODUCTION

Coal bumps are sudden, violent bursts of coal from a pillar or pillars or a block of coal, resulting in a section, the whole pillars, or the solid block of coal being thrown into an open entry with shattered coal stacking up to the roof line. Sometimes, a massive block of coal may be pushed into an open area up to 10 ft (3.1 m) without shattering or changing the original shape of the block of coal, though the block of coal may appear to be somewhat loosened up (Jahns, 1963). A bump may or may not be accompanied by an airblast and great clouds of pulverized, suspended coal dust. Coal bumps are also called **mountain bumps**, **bursts**, **outbursts**, and **bounces** depending on the coal fields. The amount of coal ejected may range from 5 to 1,500 tons (Fig. 9.1.1). A small amount of gas may also be released. However, if ejection of coal is due to the release of a large amount of highly-pressurized gas, especially methane, it is called a **gas outburst**.

Coal bumps are the results of a sudden release of elastic strain energy stored in coal pillars. They occur only in coal seams with specific geological and mining conditions. Rice (1935, 1936) stated that there are two types of coal bumps: shock and pressure bumps. **Shock bumps** occur where a strong massive stratum or strata lying immediately above or in close proximity to the coal caves as a beam or flat arch and sets up a shock wave that is transmitted downward to the coal pillar (Fig. 9.1.2). If the underlying coal pillar(s) is already highly stressed, the transmitted shock wave may cause the pillar to bump. **Pressure bumps** occur when a strong and brittle pillar is stressed beyond its strength and fails suddenly and violently.

It must be emphasized that the bumps defined above and in this chapter refers mainly to those causing fatalities and/or serious injuries. There were many more bumps, ranging from barely audible to that equivalent to 2-4 on the Richter scale that did not involve fatalities or serious injuries and went unreported and thus undocumented. Nevertheless, those fatality cases do present many phases of mining and geological conditions associated with bumps in U.S. underground coal mines.

When a longwall panel of sufficient width and length is excavated, the overburden roof strata are disturbed in order of severity from the immediate roof toward the surface. Figure 7.3.1 (p 319) shows the four zones of disturbance in the overburden strata in response to the longwall mining below.

A **B**

Fig. 9.1.1 Scenes of coal bumps. Note that the roof in both cases were undamaged and very often there is a gap between the roof and the top of the broken pillars (Boler et al., 1997; Hayduk, 1984; Newman, 2002)

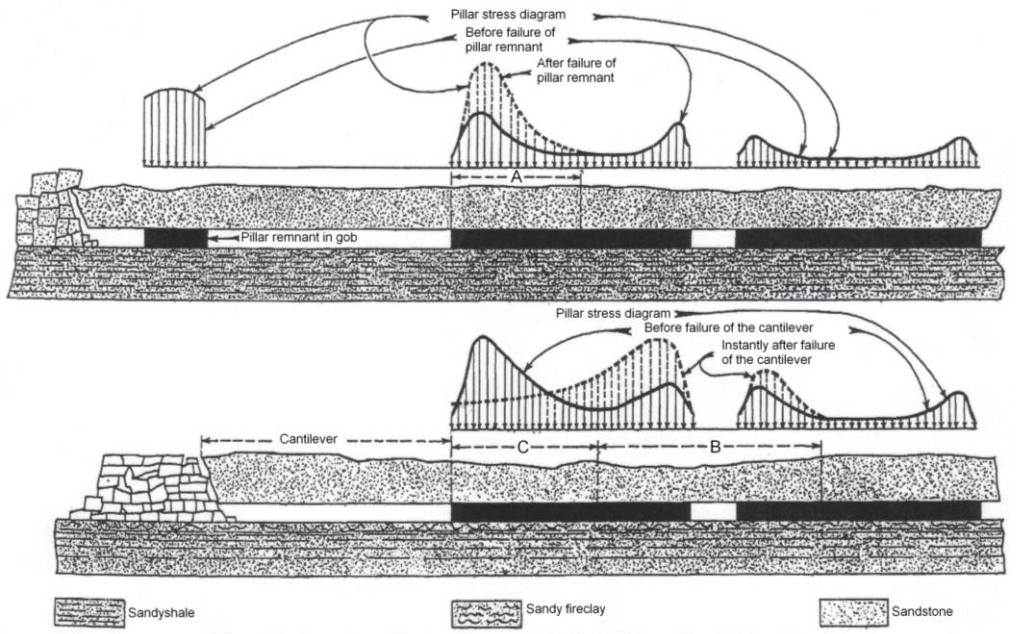

Fig. 9.1.2 Mechanisms of bumps (Holland, 1955)

9.2 OCCURRENCE OF COAL BUMPS

So far it has been generally agreed that bumps occur when the following three conditions are encountered (Agapito et al., 1988; Brauner, 1994; Campoli et al., 1987; Holland and Thomas, 1954; Holland, 1958b; Iannacchione and Zelanko, 1994; Maleki, 1995; Kripakov and Kneisley, 1992; Oyler et al., 1987; Peperakis, 1958): (1) Favorable geological conditions including (i) an overburden thickness greater than 500-700 ft (152.4-213.4 m), (ii) a strong and stiff overlying stratum or strata that overhang into the gob area, (iii) a strong and brittle coal that does not crush easily, and (iv) a strong floor rock that does not heave readily. (2) Mining methods or sequences that create localized high stress concentrations and (3) the presence of structural geological anomalies such as faults and sandstone channels. Geological conditions are by nature, whereas mining methods are artificial. It must be noted however, that shock bumps may not require the same geological conditions as stated above.

Table 9.1.1 is a compilation of rock mechanics properties of rock/coal for various cases of coal bumps reported by Campoli et al., (1989), Haramy and McDonnell (1988), Holland (1958b), Maleki (1995) and Oyler et al., (1987). It shows that, contrary to the general belief as stated earlier, a bump may occur even though one or more of those geological conditions are not present, especially that a strong roof and a strong floor do not necessarily have to be located directly above and below the coal seam. Most importantly, the key factor is that the strong roof strata must be located within the caving influence zone, say 8-10 times the mining height. In the eastern coal field, strong roof and floor were always present in seams where bumps occurred, whereas soft immediate roof and/or floor were frequently present in the

western coal field. With regard to coal, a strong and brittle coal is not a necessary condition. Bumps may occur in soft coals with a strong roof and floor. Bump-prone coals in the eastern coalfield were mainly metallurgical grade and softer than those in the western coal field.

9.2.1 Favorable Geological Conditions

1. Overburden Thickness Greater than 500-700 ft (152.4-213.4 m)

Vertical pressure exerted on a pillar is proportional to the overburden thickness. Consequently, the deeper the coal seam, the higher the pressure and the more probable that the pressure imposed on a pillar is near its fracture strength and thus will cause a bump. Rice (1935) reported that coal bumps often occurred when the overburden is 1,000 ft (304.8 m) thick or more, but they also occurred when the overburden was as little as 500 ft (157.4 m) where the surface over a specific area was rising steeply. Campoli et al., (1987) reported the seam depths of five cases where bumps caused fatalities ranged from 700 ft (213.4 m) to 2,200 ft (670.6 m).

Rice (1935) also reported that in central Appalachia the frequency of coal bumps increased during pillar extraction when the cover was more than 1,500 ft (457.2 m). It became very severe when overburden was more than 2,000 ft (609.6 m).

In Utah, MSHA will consider approval of a two-entry yield pillar system for longwall development to reduce bumps when the cover reaches 1,000 ft (304.8 m). In the Aberdeen seam in Utah, bumps began to occur when the cover reached around 900-1,000 ft (274.3-304.8 m). Frequency and magnitude of bumps continue to increase with depth until the maximum depth of 3,000 ft (914.4 m) is reached. Experience in deep mining operations indicates that bump frequency and magnitude increase with increasing cover depth.

2. A Strong Overlying Rock Stratum or Strata

Bump-prone coal seams are always overlain by a strong and stiff stratum or strata such as limestone, sandstone, or massive shale. These strata can lie either directly above the coal seam or be sandwiched by layers of soft materials 4-10 ft (1.2-3.04 m) thick (Campoli et al., 1987). However, Rice (1936) stated that the collapse of a thick conglomerate stratum caused bumps in a coal seam 1,000 ft (304.8 m) below, because the fall of a large rock mass through a small space made by the subsidence of more flexible strata below created a shock wave that traveled down to the roof of the coal seam.

In Utah where coal bumps occur in nearly all coal seams, the seams are usually overlain by competent interbedded shale, siltstone, and sandstone. There is one or more thick, massive sandstone units, 300-400 ft (91.4-121.9 m) thick, overlying those immediate roof units at various distances ranging from zero to 650 ft (198.1 m).

Iannacchione and Zelanko (1995) stated that among the 95 bump sites reviewed, 86 sites had the presence of sandstone with descriptive terms such as strong, massive, firm or thick, and that in 30 sites, a shale, sandyshale, siltstone, or mudstone layer of varying thickness is sandwiched between the overlying sandstone and coal.

Table 9.1.1 Rock mechanics properties of roof, coal, and floor of bump sites

Rock type		Uniaxial compressive strength (UCS), psi															
		Seams															
		Pocahontas #4		Harlan		Pocahontas #3	Upper Banner	Taggart	War-creek	Marker	Blind Canyon	Rock Canyon	Coal Basin	Sub-3	Wattis	Lower Sunny-side	Kenil-worth
Roof	Sandstone	24,200	14,741	14,939	13,892	24,170	17,860	15,550	19,000	×	14,489	14,939	25,085	19,000	13,329	×	×
	Sandy Shale	×	×	×	×	18,390											
	Siltstone	×	×	12,038	×	×	×	×	×	×	×	×	×	×	13,967	-	×
	Siltstone*	×	×	-	×	×	×	×	×	×	×	×	×	×	-	3,869	×
	Mudstone	×	×	×	×	×	×	×	×	×	×	×	×	×	3,422	×	×
Coal		2,400	2,743	2,756	5,138	1,798	3,011	3,122	2,178	5,862	3,263	1,100	4,642	3,000	2,654	4,541	3,642
Floor	Sandstone	21,900	×	×	×	×	×	×	×	×	×	×	×	4,003	×	-	×
	Sandstone*	-	×	×	×	×	×	×	×	×	×	×	×	×	×	8,987	×
	Shale	12,600	×	×	×	×	×	×	×	×	×	8,557	16,413	×	×	×	×
	Siltstone	16,900	7,016	16,969	9,003	×	3,488	7,587	×	×	×	×	×	×	×	×	×
	Siltstone*	-	4,191	-	5,392	×	1,250	6,298	×	×	×	×	×	×	×	×	×
	Sandstone/ Mudstone	×	×	×	×	×	×	×	×	×	×	×	×	×	7,135	×	×
	Mudstone	×	×	×	×	×	×	×	×	×	×	×	×	×	12,705	×	×

Table 9.1.1 Rock mechanics properties of roof, coal, and floor of bump sites (cont.,)

Rock type		Young's modulus, 10^6psi													
		Seams													
		Pocahontas #4		Harlan		Pocahontas #3	Upper Banner	Taggart	War creek	Blind Canyon	Rock Canyon	Coal Basin	Sub-3	Wattis	Lower Sunny-	Kenilworth
Roof	Sandstone	5.16	5.29	2.31	3.00	5.92	2.98	3.67	7.20	5.70	2.31	3.93	4.01	1.45	×	×
	Sandy Shale	×	×	×	×	5.74	×	×	×	×	×	×	×	×	×	×
	Sandstone*	-	3.708	-	-	×	-	-	-	-	-	-	-	-	×	×
	Siltstone	×	×	3.39	×	×	×	×	×	×	×	×	×	0.16	-	×
	Mudstone	×	×	×	×	×	×	×	×	×	×	×	×	0.13	×	×
Coal		0.61	0.37	-	0.567	×	0.68	0.58	0.274	0.35	0.50	0.38	0.67	-	0.487	0.654
Floor	Sandstone	5.45	×	×	×	×	×	×	×	×	×	×	2.70	×	-	×
	Shale	3.97	×	×	×	×	×	×	×	×	1.01	3.08	×	×	×	×
	Siltstone	-	-	0.29	6.20	×	1.709	4.416	×	×	×	×	×	×	×	×
	Siltstone*	-	-	×	4.60	×	-	6.466	×	×	×	×	×	×	×	×
	Sandstone/Mudstone	×	×	×	×	×	×	×	×	×	×	×	×	0.01	×	×
	Mudstone	×	×	×	×	×	×	×	×	×	×	×	×	0.22	×	×

Table 9.1.1 Rock mechanics properties of roof, coal, and floor of bump sites (cont.,)

Rock type		Tensile strength, psi						
		Seams						
		Pocahontas #4		Harlan	Upper Banner	Taggart	Warcreek	Coal Basin
Roof	Sandstone	1,070	6,653	4,833	4,686	6,233	4,510	947
	Sandstone*	-	5,106	2,615	×	-	-	-
Coal		-	-	-	-	-	-	-
Floor	Sandstone	1,010	×	×	×	×	×	×
	Shale	970	×	×	×	×	×	904
	Siltstone	1,320	2,169	2,666	1,353	3,948	×	×
	Siltstone*	×	1,734	2,037	1,354	3,786	×	×

Rock type		Poisson's ratio							
		Seams							
		Pocahontas #4		Pocahon-tas #3	Harlan	Taggart	Marker	Coal Basin	Kenil-worth
Roof	Sandstone	0.30	0.08	0.16	0.25	0.32	0.32	0.16	0.42
	Sandy Shale	×	×	0.28	×	×	×	×	×
Coal		0.31	-	-	-	-	-	-	-
Floor	Sandstone	0.39	×	×	×	×	×	×	×
	Shale	0.29	×	×	×	×	×	0.12	×

* Denote in wet condition, all others are in dry condition.

× Rock strata not applicable to that seam

- Tests are not available

Sources: Campoli et al., (1989), Haramy and McDonnell (1988), Holland (1958b), Maleki (1995), Turnipseed, (1984), and Oyler et al., (1987).

3. Coal

Coal bumps are known to occur in the eastern and western coal fields: the metallurgical grade coal seams such as Pocahontas, Harlan, and Darby seams in central Appalachia; most seams in the Somerset coal field in Colorado; and all seams in the coalfield of central Utah.

Rice (1935) reported that the Harlan and Darby seams in Kentucky, where bumps occurred in the early 1900s, are strong, high-grade, high volatile gas coals with pronounced development of face and butt cleats. Brauner (1994) stated that rockbursts occurred in seams with 12-38 % volatile matter with an average of 23 %, that rockbursts never occurred in seams with less than 10 % of volatile matter, and that rockbursts occurred in coal seams with UCS ranging from 725.2 to7,251.9 psi (5 to 50 MPa).

Coal's susceptibility to bursting is related to its mechanical properties. Since a burst is a sudden manifestation of the release of stored elastic strain energy, the tendency of the coal to burst depends on its ability to accumulate elastic strain energy. It decreases as the permanent strain increases. This can best be illustrated by a coal specimen subjected to uniaxial compression (Fig. 9.2.1). The coal specimen is loaded to about 80 % of its ultimate strength and unloaded. Upon complete unloading, strain does not return to the original zero strain condition; rather, various amounts of strain remain, which are called plastic or permanent strain. The total energy imparted to the specimen for the stress-strain curve AB is E_t, made up of two components: one is elastic strain energy E_e, which is released immediately upon release of the applied stress, and the other one is the permanent strain energy E_p, which is irrecoverable upon release of the applied loading. Permanent strain energy is energy used for grain loosening, crack propagation, intergrain friction and so on (Neyman et al., 1972).

Coal's tendency's to bump can be expressed by a **burst energy index** W_{et}, which is the ratio of elastic strain energy accumulated in the specimen to the permanent strain energy (Neyman et al., 1972).

$$W_{et} = \frac{E_e}{E_p} = \frac{\int_{\varepsilon_p}^{\varepsilon_t} f_1(\varepsilon\varepsilon)d}{\int_0^{\varepsilon_t} f_1(\varepsilon\varepsilon)d\varepsilon - \int_{\varepsilon_p}^{\varepsilon_t} f_1(\varepsilon\varepsilon)d} \tag{9.2.1}$$

where ε_t and ε_p are total and permanent strains, respectively. The larger the value of W_{et}, the greater the susceptibility to bumps. Using this index, coal's susceptibility to burst can be classified as follows:

Degree of bump susceptibility	W_{et}
Severely susceptible	> 5
Slightly susceptible	2 – 5
Not susceptible	< 2

Brauner (1994) also showed that coal of low to medium strength 1,523-2,147 psi (10.5-14.8 MPa) and stiffness of E = 1.5 x 105 - 2.4 x 105 psi (1,050-1,680 MPa) exhibited heavy bursts, and that the burst energy index is a more reliable indicator of whether a coal is liable to bump. The UCS of all coal seams where bumps causing fatalities and serious injuries ranged from 1,100 to 5,862 psi (7.58-40.42 MPa) (Table 9.1.1).

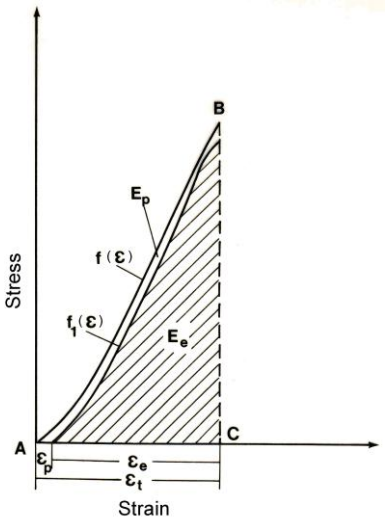

Fig. 9.2.1 Terminology used in the burst energy index (Neyman et al., 1972)

A coal seam and its thickness do not seem to affect bump occurrence. Bumps have been reported in at least 25 coal seams in four eastern states (Alabama, Kentucky, Virginia, and West Virginia) and two western states (Colorado and Utah), and their thickness ranged from 43 in. (1.09 m) to 14 ft (4.3 m) (Campoli et al., 1987; Iannacchione and Zelanko, 1995; Peperakis, 1958). However, Agapito and Goodrich (2000) stated that thinner seams induced higher vertical stress in the tailgate than the thicker seam. There was no bump in the thicker seams while severe bumps occurred in the thinner seam.

4. Floor Strata

In the eastern coalfield, all bumps occurred in coal seams with hard or firm immediate floor, although in some cases, the immediate floor strata were soft but thin and underlain by thick strong strata. If the floor is soft and thick, a pillar is likely to punch into a floor that is softer than the pillar itself and dissipate energy stored in the pillar. Brauner (1994) stated that not all bumps occurred in a strong floor. Iannacchione and Zelanko (1995) stated that hard and dense shale floor was the predominant rock type, while the presence of sandstone is noted in only 25 % of the site descriptions.

There are indications that the thickness of a strong floor is an important parameter. If a strong floor of limited thickness is underlain by a weak and soft stratum, excessive pressure coming from the overlying pillar will tend to squeeze out the soft stratum and may eventually rupture the strong immediate floor and induce bumps (Haramy et al., 1985; Rice, 1936; Turniseed, 1984).

9.2.2 Mining Methods and Cutting Sequences

There are two major underground mining methods in the U.S. (see Section 1.2 on p. 3), longwall mining and room and pillar mining. Bumps occurred in both mining methods in the eastern and western coalfields. U.S. longwall panel layout has been standardized, and once the individual panels are developed, it must be rigidly followed and changes are not feasible without suffering great production and economic losses. Room and pillar mining, on the other

hand, is very flexible; panel layout and mining sequence can be changed almost any time without suffering much production and economic loss. Consequently, bumps that occur in longwall panels cannot easily be dealt with by changing the overall panel layout, as compared to room and pillar mining where more options exist regard to pillar layout and cutting sequences.

1. Longwall Mining

In longwall mining, coal bumps generally occurred in the tailgate chain pillars adjacent to, and due to the side abutment created by the previous gob except when yield pillars are used (Agapito et al., 1988; Barron, 1990; Kripakov and Zelanko, 1992). Bumps also occurred at the longwall face near the tailgate end and the panel ribs of the tailgate within 60-100 ft (18.3-30.5 m) outby the tailgate T-junction, again due to the heavy pressure resulting from the overlapping of the side abutment from the previous gob and the front abutment from the current advancing longwall face. Table 9.2.2 shows the percentage of bump occurrence in both locations (Iannacchione and Zelanko, 1995). Over 95 % of the bumps occurred greater than 1,000 ft (304.5 m) from either end of the longwall panels, and no seismic events were observed until the distance to the side boundary of the section exceeded 4,000 ft (1,200 m) (Ellenberger and Heasley, 2000).

Table 9.2.2 Percentages of location of bumps

Longwall					Room and pillar		
Face	Tailgate entry	Face & tailgate	Headgate	Others	Pillar retreat	Barrier splitting	Development
33	19	36	6	6	47	35	18

There are two methods used to alleviate chain pillar bumps and bump hazards in the tailgate, as well as headgate in some cases: the two-entry yield pillar gateroad development system in Utah and the yield-abutment or yield-abutment-yield gateroad development system in the Appalachian coal field. The two-entry yield pillar system is very successful in alleviating chain pillar bumps (Agapito et al., 1988; Kripakov and Kneisley, 1992). More detailed description about occurrence and control of bumps in longwall mining is discussed in Section 9.5 on p.447. For details about yield pillar design and its function refer to Section 9.5.1 on p. 448 and Section 5.4 on p. 260.

2. Room and Pillar Mining

In room and pillar mining, retreat pillar mining was the major cause of coal bump, followed by barrier splitting and development (Table 9.2.2). There are various methods employed for retreat mining of chain pillars in production panels (Feddock and Ma, 2006; Kaufman et al., 1981). Depending on the method and sequence of cutting selected, the percentage of recovery for each pillar, and thereby the pillar line, varies from time to time. Consequently, certain pillars may receive higher loads transferred from others that are being cut. The additional load transferred may be sufficient to bring the total loading on the already highly-stressed pillars to exceed their strength, leading to bumps of those pillars.

Pillar retreat creates abutment zones and pressures around the periphery of the gob, resulting in loading conditions very similar to longwall mining depending on the percentage of

recovery. The abutment zone extends approximately 200-500 ft (61-152.4 m) ouby the pillar line (Hayduk, 1984; Holland, 1958b). Within this zone, pillar configuration, and consequently, cutting sequence must be strictly followed such that it does not overstress any particular portion of a pillar or pillars (Iannacchione and Zealanko, 1995). Figure 9.2.2 shows an example of bumps of pillars during retreat mining (Campoli et al., 1987). Numerical numbers in the figure show the approximate sequence of cutting prior to bumps. The bumped pillars are shown as A, B, and C. Approximately 300 tons (267.9 metric tons) of coal were ejected and a miner was slightly injured. Immediately prior to the bumps, the rows of pillars that bumped were exposed to gobs on one to three sides, and took extremely high abutment loads from the overhanging sandstone roof in the gobs, causing the bumps.

Fig. 9.2.2 An example of bump in pillar extraction (Campoli et al., 1987)

Since barrier pillars are used to isolate active panels or entries from the gob, barrier splitting normally occurs at the end of mine life or sections enclosing the barriers. As such, barrier pillars are surrounded by gobs on more than one side, and during retreating operation, more than two sides. Therefore, stresses on the barrier pillars are much higher than during development. Consequently, barrier splitting must be carefully planned to make sure that the

act and sequence of cutting will not trigger bumps. Figure 9.2.3 shows a case of coal bump while extracting a barrier pillar block (Peng, 1986). The sequence of pillar splitting followed the numerical sequence of the room numbers. After completing two bump cuts (i.e., BC2 and BC3) in room 1, the CM was trammed to room 6 to complete the room development. When the CM was loading coal onto the shuttle car at the face area of room 6, the bump occurred. The coal was ejected from the ribs of the larger pillar and piled up on the floor 3 ft (0.9 m) high in rooms 1 and 6. The roof and floor were intact. A large gap occurred between the top of the coal pillar and the roof between rooms 1 and 6. The continuous miner and shuttle car in room 6 were pushed until they were against the other side of the ribs. The same thing happened to the roof bolter in room 1. The barrier pillar being split was surrounded by gobs on two sides and took two overlapping abutment loads.

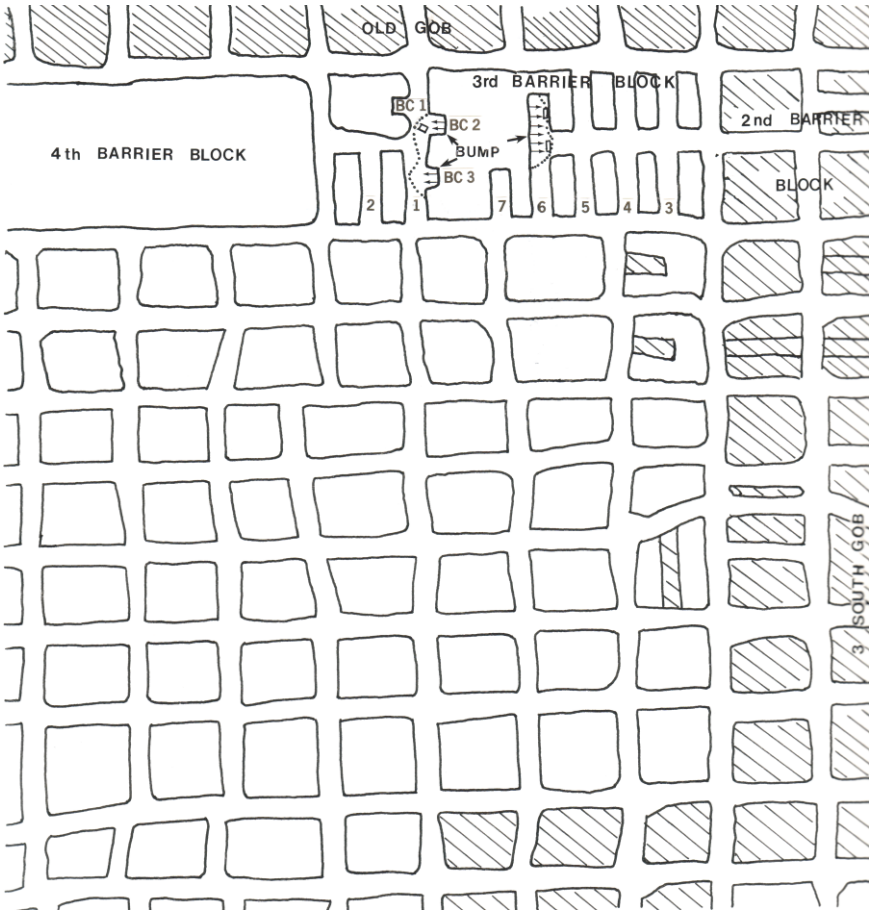

Fig. 9.2.3 An example of bump occurred during barrier splitting (Peng, 1986)

Barrier splitting was more common during the first half of the 20th century. However, its use has decreased considerably in the past two decades due to its inherent danger.

Development mining refers to the extension of entries and crosscuts into the unmined portion of the reserve. Bumps occurred when development work was close to a gob section or sections and near faults (Iannacchione and Zelanko, 1995).

3. Multiple Seam Mining

Multiple-seam mining, if not properly planned, is known to cause seam interaction resulting in areas of high stress concentration in either one or more seams. High stress concentration may cause bumps (Campoli, 1987; Iannacchione and Zelanko, 1995; Maleki, 1995; Newman, 2002; Peng, 2007). For detailed discussions on the occurrence of multiple-seam interaction, and severity of interaction, refer to Chapter 8 Multiple-Seam Mining on p. 390. It must be emphasized, however, that in order to quantify and pinpoint the effect of interaction of certain mining layouts in the interacting seams, detailed stress analyses must be performed on a case by case basis.

Newman (2002) reported on two cases of bumps during upper seam mains development (Fig. 9.2.4). Both seams were mined by the room and pillar method with interburden 140-160 ft (42.7-48.8 m) thick consisting of strong and competent sandstone (approximately 100 ft or 30.5 m thick), sandy shales, interbedded sandstone and shale, and shales. The lower seam was 1,450-1,700 ft (442-518.2 m) deep and mined first. No precursor events occurred prior to the first bump. There were numerous small bumps preceding the second bumps that involved 6 pillars two blocks outby the development face. The bumps were attributed to stress concentration at the edges of the barrier pillars in the lower seam.

In Utah Wasatch Plateau, a two-seam longwall mine was conducted with an interburden 80 ft (24.4 m) thick consisting of strong and competent sandstone and sandy shale under an overburden of up to 1,600 ft (487.9 m) (Peng, 2007). Columnization was used to lay out the mine plans in both seams. In the lower seam, stress concentration caused by the barrier pillars in the upper seam often caused floor bumps. Experience showed that columnization under large overburden thickness was not good, because the upper seam remnant pillars would transmit high pressures to damage the lower seam pillars and entries.

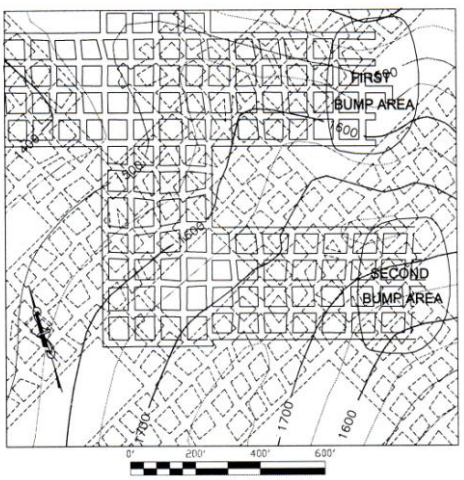

Fig. 9.2.4 Bumps in the upper seam development faces due to multiple-seam interaction involving room and pillar mining in both seams (Newman, 2002)

9.2.3 Presence of Structural Anomalies

Structural anomalies that have been found to be associated with bumps are faults and sandstone channels (Agapito and Goodrich, 2000; Peperakis, 1958; Iannacchione and Zelanko,

1995). Faults are known to be associated with ground control hazards. Most faults cause roof falls. Peperakis (1958) reported six cases of violent bumps from 1918 to 1957 that occurred when the face was close to, at, and passed the faults. Bumps also occurred between two faults that intersect to form a wedge block, but did not occur beyond this block (Watts, 1918).

Sandstone channels, when they were located 10-20 ft (3.05-6.1 m) above the coal seams, had been found to be associated with bumps at the longwall face less than 1,000-1,200 ft (304.8-365.8 m) of cover in the bump-prone coal mines of Utah. Bumps did not normally occur less than 1,500 ft (457.2 m) cover without the presence of sandstone channels.

Figure 9.2.5 shows three cases of bumps believed to be associated with sandstone rolls (Iannacchione and Zelanko, 1995). The first one (May 1978) occurred in the first row of chain pillars at the headgate T-junction. The second one (March 1980) involved six small pillars. The exact location of the third bump (July 1980) could not be accurately determined.

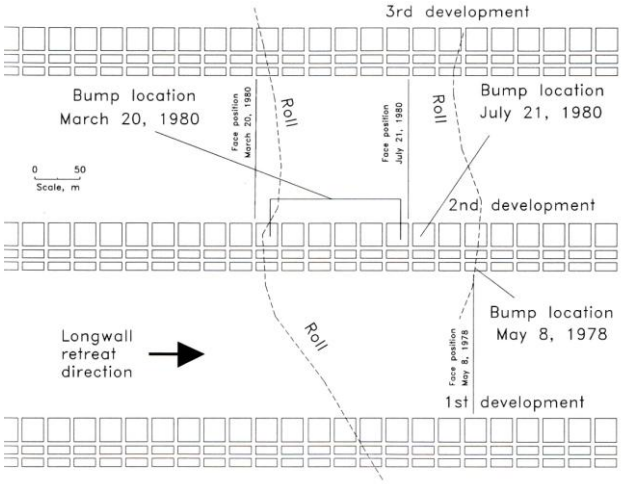

Fig. 9.2.5 Bumps associated with sandstone rolls (Iannacchione and Zelanko, 1995)

9.3 CAUSES AND MECHANISMS OF COAL BUMPS

Coal bumps are a manifestation and result of the sudden release of energy stored in coal under high stress. Several theories have been proposed (Babcock and Bickel, 1985; Holland, 1958b; Iannacchione and Zelanko, 1994; Maleki, 1995; Rice, 1935) regarding the sources for bumps. But the mechanisms of coal bumps and how the energy stored in coal is released are still not well understood.

9.3.1 High Static Stress Concentration

This group of theories follows the traditional, most commonly accepted concept that states when the applied stress exceeds the strength of coal, a pillar fails. In underground coal mining, when coal is removed, the overburden load originally supported by the excavated coal will be transferred to other parts of the mine structure (e.g., chain or barrier pillars or solid coal blocks) surrounding the area of excavation. The areas to which the load transferred and the magnitude and distribution of the transferred load depend mainly on the mine layout and sequence of mining. So in this theory, emphasis is placed on identifying the sources and

determining the magnitude and distribution of stress concentration on a pillar or group of pillars surrounding the excavated area (Campoli et al., 1989; Holland, 1955 and 1958b; Maleki, 1995; Rice, 1935).

In underground mining, a large load transfer can be generated by mine layout: abutment pressures around the edges of a longwall panel and mined out gob in pillar extraction panels (Figs. 9.2.2 and 9.2.3), stress concentration resulting from pillar columnization and gob/solid coal (or solid rock) boundaries in multiple-seam interaction (Fig. 9.2.4).

The criteria for bump initiation varied with individual research. Most believed that when the average stress in the pillar exceeds the estimated pillar strength, bursts occur (Campoli et al., 1987; Holland, 1958b; Maleki, 1995; Rice, 1936). Pillar strength can either be estimated from laboratory uniaxial compressive strength tests of coal specimens or determined by field measurement (Agapito et al., 1988; Maleki, 1992). The use of average pillar stress tends to ignore the non-uniform stress distribution in the pillar due to frictional constraint at the coal/roof and/or coal/floor, and non-homogeneity in the coal seam (Babcock and Bickel, 1983; Holland, 1958b; Meikle, 1965; Peng and Johnson, 1972). A pillar under confinement is stronger than under uniaxial compression, as simulated in the laboratory by uniaxial compressive strength tests. In fact, coal strength increases with increasing confining pressure until it reaches the brittle to plastic transition. Holland (1958b) termed the strength of coal as **ultimate strength** when it first reaches the plastic stage. Since stress distribution in underground pillars is rarely uniform, pillar strength in various parts of the pillar also varies as a result of varying degree of confinement. However, triaxial pillar strength was only considered in a few cases for bump analysis (Heasley and Zelanko, 1992).

Maleki (1995) went further with his stress criteria using five case studies. He identified stress factors that caused bumps; (1) there are induced horizontal stresses in the pillar, so the pillar strength is larger than the UCS. Variation of horizontal stresses during mining help the pillar, after failure, to unload in a stable manner. (2) when cover increases rapidly over a short distance and mining also proceed rapidly in a short period of time, a marginally stable pillar will fail violently. (3) a critically loaded pillar can be triggered to bump by failure of the upper strata as much as 300 ft (91.4 m) above the coal seam. (4) lack of yielding in the floor promotes pillar confinement, thereby potential for bumps. And (5), bumps can be avoided with the presence of cleated coal, yielding floor, and sharp contact conditions of interface between coal and roof.

9.3.2 Dynamic Stress Concentration or Shock Wave

Rice (1936) proposed this mechanism and called it a shock bump due to the breaking of thick, massive, rigid strata at a considerable distance above the coal seam, causing a great hammer-like blow to be given to the immediate roof, which is transmitted as a shock wave to the coal pillar or pillars.

No work has been done to advance this theory. Maleki (1995) stated that this mechanism was a contributing factor to bumps when a strong, stiff, and jointed sandstone caved periodically. The sandstone was 200-300 ft (61-91.4 m) thick lying 300 ft (91.4 m) above the coal seam.

9.3.3 Constraints at the Interface of Coal/Roof and/or Coal/Floor

Laboratory experiments by Meikle (1965), Khair (1968), Peng (1970), and Peng and Johnson (1972) have clearly demonstrated that different interface conditions or coefficients of friction

between coal and roof and between coal and floor will produce different ultimate strengths, uniaxial or triaxial compressive strengths, for the same rock or coal specimens (see Section 2.6.1 on p. 53). Coal or rock strength increases with increasing interface friction because the frictional constraint creates a triaxial state of stress in the specimen within its influence zone, which is related to specimen width. The confining pressure generated will increase the material strength. Since the influence zone of the interface friction is limited, slender pillars, i.e., those specimens with higher ratios of width to height, may not be subjected to a triaxial state of stress around their mid-height area, leading to lower strength.

Peng (1970) derived analytical solutions for stress distribution in cylindrical specimens subjected to uniaxial and triaxial compressions under various interface friction conditions between specimen and machine platens. When interface friction is high, more specimen volume is subject to a high triaxial state of stress (see Section 2.6.1 on p. 54).

Holland (1958b) stated that brown stains on the roof (fine coal dust) and slickensiding, common to burst sites, indicate that a relative movement at the interfaces between the pillar and roof and/or between coal and floor has occurred and suggested that bumps may be initiated by some action that causes a change in the coefficient of friction between coal and its adjacent strata. Meikle (1965) demonstrated in the laboratory that when friction at the interface is reduced, coal strength is also reduced. The implication is that when a coal pillar is loaded close to its ultimate strength under constraint conditions, a sudden reduction of interface friction due to various reasons (e.g., moisture penetration, gouging, etc.), then pillar strength is reduced instantaneously due to sudden loss of interface constraint, resulting in bumps. Red colored material has been observed at many bump sites and described by practitioners. Several descriptive terms have been used, including “dusting of red coal” (Iannacchione and Zelanko, 1994), “red dust” (Maleki, 1995), “reddish brown coal” (Newman, 2002), and “reddish tint” (Peng, 2007) (Fig. 9.3.1). Brauner (1994) stated that blasting performed for de-stressing induced vibrations that may affect the friction between the coal and surrounding strata and that may have far-reaching effect.

Anecdotal sources emphasized that once a large block of coal has been overstressed, it will show a reddish tint in the coal. This burnt appearance may appear in the coal next to the roof or along the fracture planes where a rib rolls off the pillar. This reddish tint may be present over the entire working area. If a large pillar shows this reddish color, and it is located in the abutment zone, a decision must be made: shall the pillar be left as a bump block, or shall it be attacked and de-stressed? A bump block in the gob is strong enough to break the massive sandstone roof and create a good fall. If the reddish tint is showing in the entire area, it may be necessary to abandon all the pillars in the abutment zone. The section would drop back a distance of 4 or 5 rows of pillars and begin retreating again (Hayduk, 1984). The abutment zone is defined as the area within 200-500 ft (61-152.4 m) outby the pillar or gob line.

Iannacchione (1990) assumed that the rock/coal interface follows the linear Coulomb friction model without limit for the interfacial shear stress. Coal was simulated by the linear Mohr-Coulomb model with strain softening. Once the pillar is formed and loaded, slip at the rock/coal interface will occur when the critical shear stress is reached, decreasing the horizontal stress along the interface. Consequently, the pillar loses the confinement at those slipped portions, which yields and transfers stress toward the solid core of the pillar. The process of interface slippage, loss of confinement, and stress transfer continues until the pillar reaches equilibrium or completely yields. Analysis of stress profiles at different interface cohesions shows that the gradient of vertical stress within the yielded zone is greatly affected by the interface properties (cohesion and friction angle). The width of the yield zone is

inversely, while the magnitude of the peak stress is directly, proportional to interface cohesion. The pillar strength is directly proportional to cohesion and friction angle.

A bi-linear Coulomb friction model was used by Morsy (2003), based on the direct shear test of coals obtained by Peng et al., (1983) to simulate the rock/coal interface. Sliding will occur if the magnitude of the interfacial shear stress reaches a certain limit. The vertical and horizontal stress distributions within the yield zone of the pillar are independent of the overburden depth because when the pillar ribs start to yield, the coal pillar/rock interface deteriorates at the yield zone. Hence, the degree of confinement at the yield zone will be independent of overburden depth. This behavior cannot be achieved by using the linear Coulomb friction model for the coal/rock interface. The linear coulomb friction model predicts a higher frictional resistance with higher overburden depth. Consequently a higher vertical and horizontal stress will occur even in the yield zones. With the bi-linear model, however, a completely yielded pillar could be achieved by using a small shear limit

Fig. 9.3.1 Red dust at the roof of the bump sites (see color photos in Appendix 3)

Babcock and Bickel (1984) collected coal samples from 11 coal seams in six states and conducted uniaxial compression tests on model pillars with a width-to-height ratio of 8.5. The experimental setup was such that friction between coal and machine platens would change as the applied load approached the load of failure. 13 of the 15 coal seams tested were made to burst including those that did not have a history of coal bumps. They concluded that many, if not most, coals can be made to burst given the necessary conditions of stress and constraint. The constraint can be lost dynamically to produce bursts, while the unconstrained strength cannot be lost.

Holland (1958b) also found that pillars fail violently when the width/height ratio is low and tend to fail gradually when the width/height ratios are larger, and that the width/height ratio at which coal's transition from violent to gradual failure increases with coal strength (Table 9.3.1). Due to interface constraint, stress distribution in the pillar is non-uniform. Yielding occurs at the ribs, and depth of yielding varies. Vertical stress is zero or low at the rib side and increases with depth into the pillar. The rate of stress increase also varies with constraint. If the high stress zone is shallow, it will bump upon cutting into it. Pillars with low width/height ratio are subjected to less constraint in volume and more likely to fail violently. The reverse is true for pillars with large width/height ratios.

Conversely, Brauner (1994) stated that in Ruhr mines, bursts occurred only when the width-to-height ratio was between 8 and 20.

Table 9.3.1 Effect of width/height ratio on pillar's failure mode (Holland, 1958b)

Coal seam	UCS[1]		Width/height ratio	
			Failure mode	
	psi	MPa	violently	gradually
Beckley	1,163	8.02	< 2.85	2.87-4.9
Island Creek	4,725	32.58	6.7	6.8
Hernshaw	4,725	32.58	6.85	9.61
Coalburg	6,861	47.31	7.82	12.0

[1] Uniaxial compressive strength of 3-in. (76.2 mm) cubical specimens

MSHA's (Gauna and Phillipson, 2008) investigations showed that pillar bumps have occurred in conditions of high overburden or high stresses, and strong, rigid roof and floor when pillars are in the range of 60 ft (18.3 m).

9.3.4 Local Mine Stiffness

It has been well-established in the laboratory that when a soft testing machine is used for compression tests, specimens tend to fail violently once the peak load is achieved. Whereas, under a stiff testing machine, the same specimen will fail gradually in a stable manner (Peng and Podnieks, 1972). If pillars are to fail gradually, **local mine stiffness**, defined as an equivalent stiffness of the roof, coal, and floor strata in different areas of the mine at different stages of mining (Salamon, 1970), must be larger than that of failed coal. Conversely, if mine stiffness is less than that of failed coal, violent failure will occur.

Stated differently, when coal is unable to absorb the total energy released by the surrounding rock strata during the failure process, coal will fail violently. Fig. 9.3.2 illustrated this concept (Kripakov and Kneisley, 1992). Mine stiffness is represented by parallel loading lines and decreases from very high (i.e., vertical) in stage 1 to very low in stage 4 (Fig. 9.3.2A), in which the energy released by the mine is much larger than the failed pillar can absorb, leading to violent failure (Fig. 9.3.2B). This is similar to the laboratory UCS testing in that the mine roof released its stored energy to the underlying critically loaded coal pillar causing it to fail violently, because the local mine stiffness is smaller than that of the pillar at the stage of failure initiation.

Morsy and Peng (2002a) used the local mine stiffness criterion to explain a large mine collapse in the lower Cedar Grove seam in West Virginia. In their study, the local mine stiffness varied with individual pillars located at different parts of the panel. Stiffness also is not uniformly distributed within a pillar due to non-uniform distribution of vertical stress and roof-to-floor convergence across the pillar width, being larger near both ribsides with exponential decay toward the pillar center.

In coal bumps, the roof normally remained intact and a gap of varying widths occurred between the top of the pillars and roof after bumps had occurred (Boler et al., 1997; Hayduk, 1984; Newman, 2002).

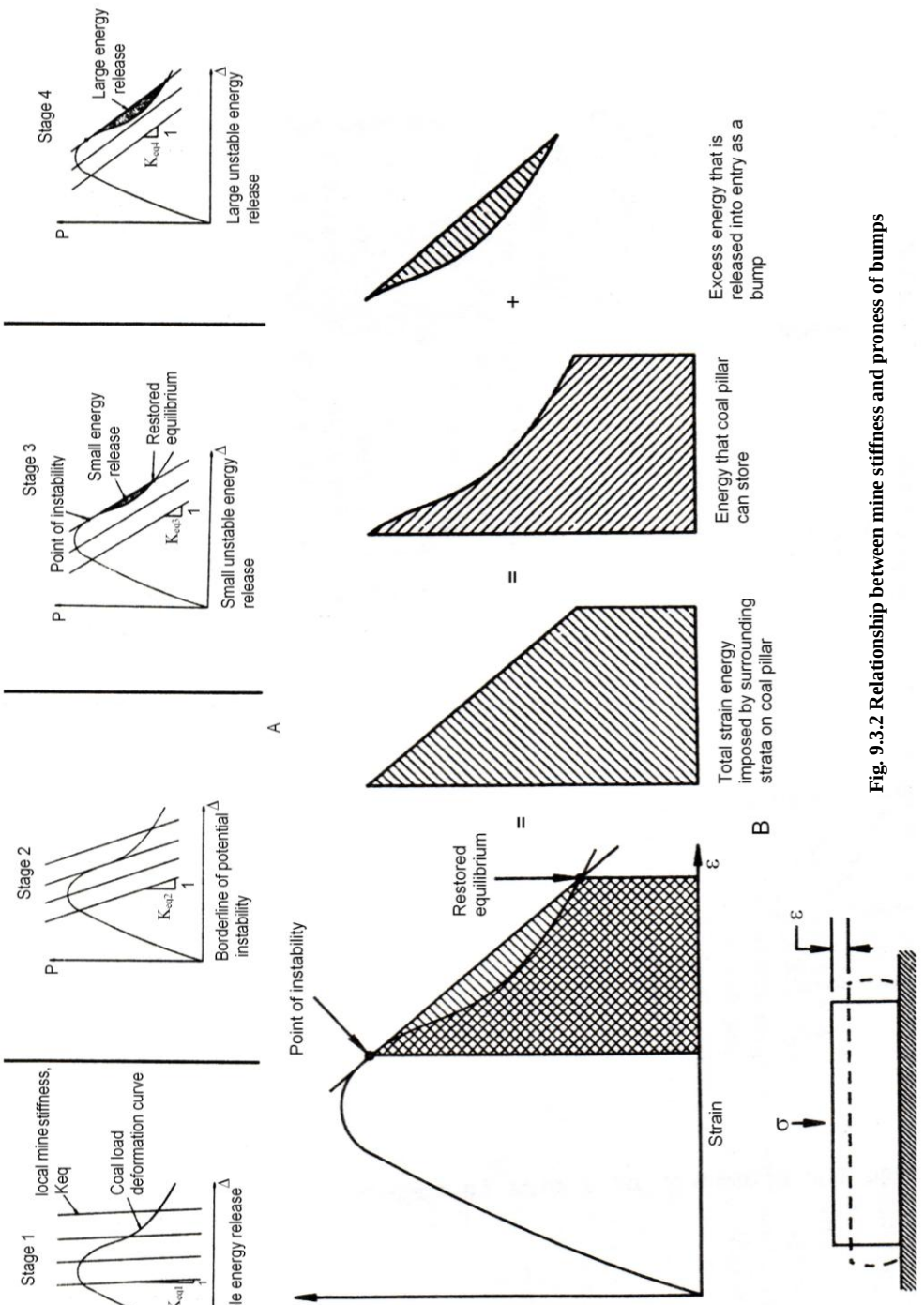

Fig. 9.3.2 Relationship between mine stiffness and proness of bumps

9.3.5 Seismic Events

Coal bumps are frequently associated with seismic events that are sufficiently large to be registered by regional seismic networks. Coal bumps are only one set of mining induced seismicity, so not every coal bump generates a regional seismic event.

Heasley et al., (2001) and Ellenberger and Heasley (2000) monitored the seismic activity of longwall mining at Willow Creek mine, Utah more than 2,500 ft (750 m) deep. The immediate roof was interbedded thin mudstone, siltstone, and sandstone. The Castlegate sandstone, 400-600 ft (121.9-182.9 m) thick was 650 ft (198.1 m) above the coal seam. They found that a majority of the seismic events were a direct result of the advancing face and that the seismic activity was mostly located in advance of the face area, 1,000 ft (304.8 m) in front of and behind and 650 ft (198.1 m) above and below the face. Seismic events were heavily clustered within 330 ft (100.6 m) in front of and behind, above and below, the face (Fig. 9.3.3). The tensile failures in the gob were not recorded due to its low energy release and high attenuation rate. A Richter 4.2 event was identified 500-600 ft (152.4-182.9 m) above the coal seam implicating the breakage of the Castlegate sandstone, causing no damage at the mine level.

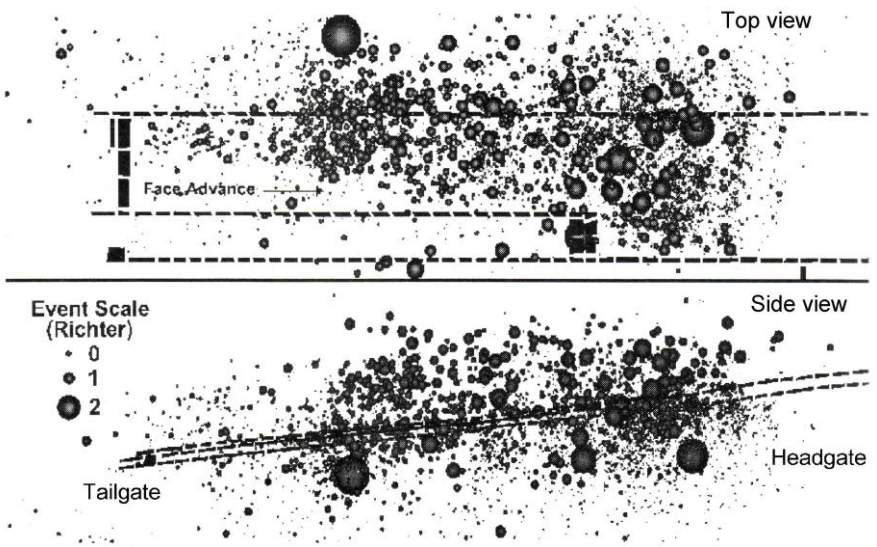

Fig. 9.3.3-D view of seismic events showing location with the event size scaled by magnitude (Heasley et al., 2001)

X Luo et al., (1998) monitored seismic events associated with longwall mining in weak and intermediate strata. They found that in weak strata an accurate fracturing zone is 0-230 ft (0-70 m) ahead of the face slightly above the seam level. The fracture zone passes obliquely at about 50^{o} from the horizontal back over the face (Fig. 9.3.4). Reverse faulting of shear fractures dominate. Very few events occur in the gob where tensile failure dominates.

In intermediate strata, the same accurate fracturing zone of 0-230 ft (0-70 m) ahead of the face is also apparent (Fig. 9.3.5), except it skews toward the tailgate. Seismic events are clustered in front of and below the face. An arc line confining the front of an extensive fracturing zone is apparent.

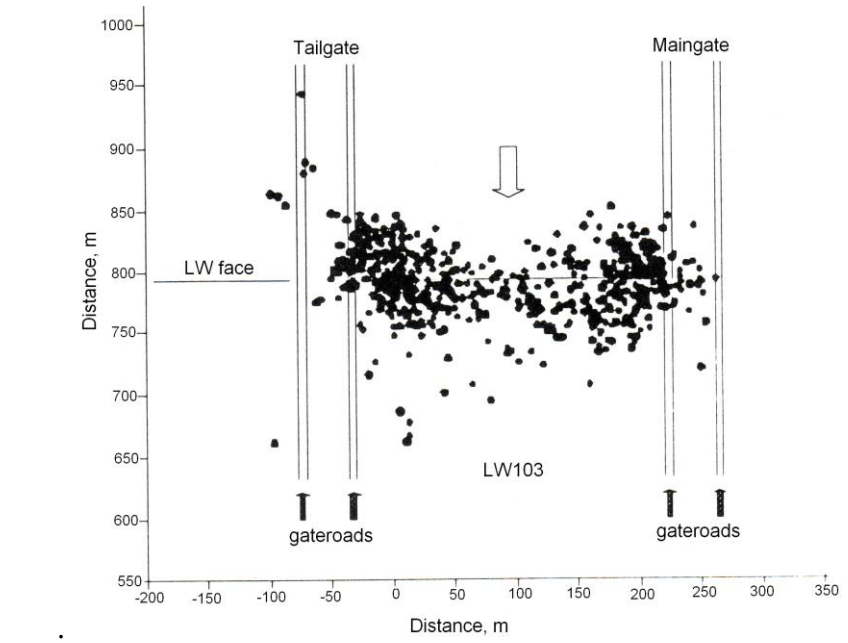

A

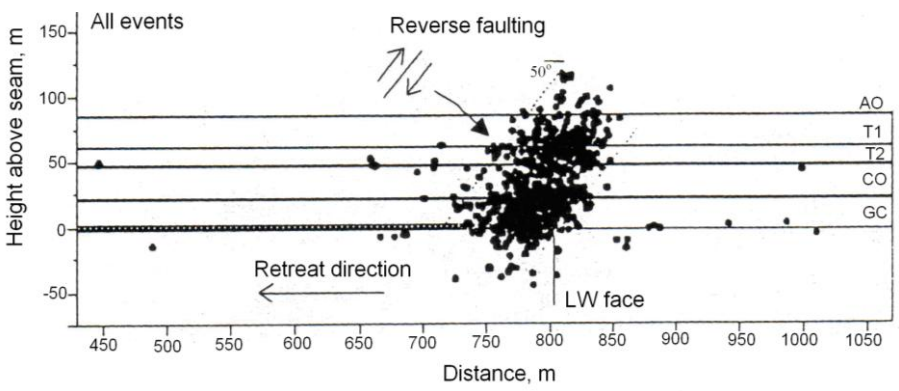

B

Fig. 9.3.4 Seismic events for longwall mining in weak strata: A, plan view B, cross-sectional view (X Luo et al., 1998)

Considering that many registered events during longwall retreat were quite large, i.e., 1.3-2.4 on the Richter scale, Maleki et al., (2003b) modeled slip along joint sets with a surface area of 80 x 400 ft (24.4 x 121.9 m). They found that the contribution of joint slip to seismicity varies with the stiffness and position to the longwall gob of the host strata, number of mined panels, and face location.

Two types of seismic events were recorded in U.K. multiple-seam longwall mines (Kusznir et al., 1980). Type A events were dilational or tensile in origin due to collapse of roof layers above the working face. The events could be attributed to reduction of the compressive principal stress in the gob, resulting in tensile failure of layers subject to reduced confinement.

They generally occurred in the gob of the panel being mined. Some occurred behind the advancing face, while some occurred in the old gobs of the upper seam 558 ft (170 m) above. Type B events were shear in origin and must occur through shear fracture of an exposed volume of rock. They occurred mainly in front abutment zones approaching the edges of pillars in the upper seam and, to a lesser extent, in the lower seam 49 ft (15 m) below.

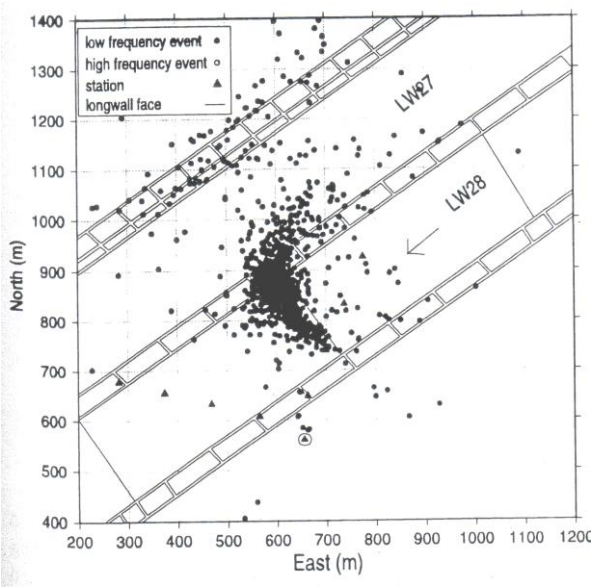

A

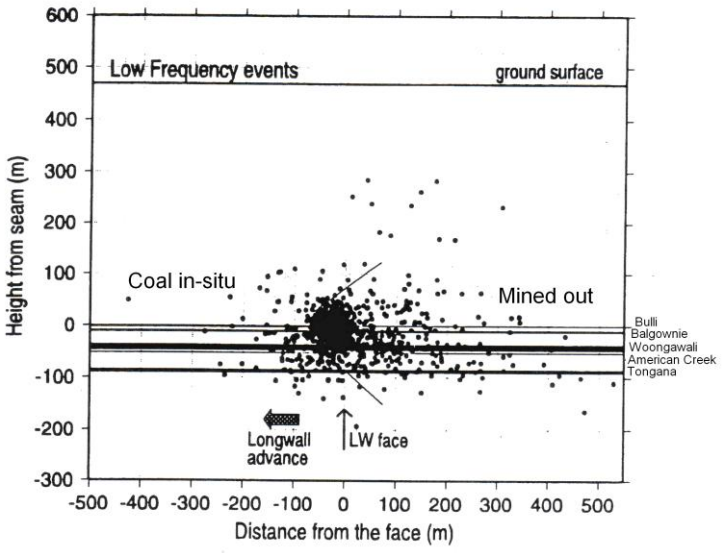

B

Fig. 9.3.5 Seismic events for longwall mining in intermediate strata: A, plan view B, cross-sectional view (X Luo et al., 1998)

9.3.6 Energy Release Rate (ERR)

Energy stored in a mine structure changes during mining. Parts of the change remain in the system, while others are dissipated or released. The latter may appear as dynamic energy-causing bumps (Heasley, 1991; Maleki et al., 1987; Zipf and Heasley, 1990).

Heasley (1991) used a strain-softening coal model (Fig. 9.3.6) for energy calculations following the coal cutting sequence. In this model, the strain energy consists of three parts: total, recoverable, and dissipated strain energies. The coal is initially loaded along AB and accumulates elastic strain energy of ABC, which is completely recoverable upon unloading. After failure with residual strength DE, any unloading will follow the line EF, parallel to AB. Thus the recoverable strain energy at E is equal to area EFG, while the total strain energy applied is ABDEG. The difference, area ABDEG – area EFG, is the dissipated energy, which is liberated to the environment.

MULSIM/NL (Zipf, 1992) was used to calculate three-dimensional stresses and displacements of a pillar extraction case in West Virginia where bumps occurred frequently. The increase in dissipated strain energy between two consecutive cutting steps was calculated. Any increase in dissipated energy implies that energy was dissipated to the environment, and that the larger the increase in dissipated energy between cutting steps, the more likely that the energy will be dissipated dynamically as a coal bump. The results showed that peak dissipated energy correlates with bump events.

Maleki et al., (1987) used computer code EXPAREA (St. John, 1978) with elastic-plastic (Fig. 9.3.7) and strain-softening (Fig. 9.3.6) models applied to a pillar extraction case in Utah where two bumps occurred. The energy release was calculated by using the following equation (Hardy and Christianson, 1977)

$$E = \frac{1}{2}\sum_{i=1}^{n}\sigma_i(\delta_{iB} - \delta_{iA})A_i \qquad (9.3.1)$$

where A_i is the area of each element, σ_i is precut stress on coal element i, δ_{iA} is closure at element i after cut is made, and δ_{iB} is closure at element i before the cut is made. The energy release was calculated for those elements that are mined during any particular mining cut. Critical levels of stress, closure, and release energy associated with bump prone conditions were determined using mining geometry prior and subsequent to the occurrence of the bump (Table 9.3.2). Modeling results showed that variation of cutting sequence do not significantly reduce the potential for coal bumps during pillar mining due to a narrow panel width.

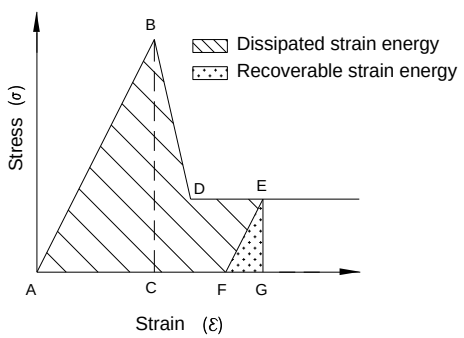

Fig. 9.3.6 Strain softening coal model for energy calculations (Heasley, 1991)

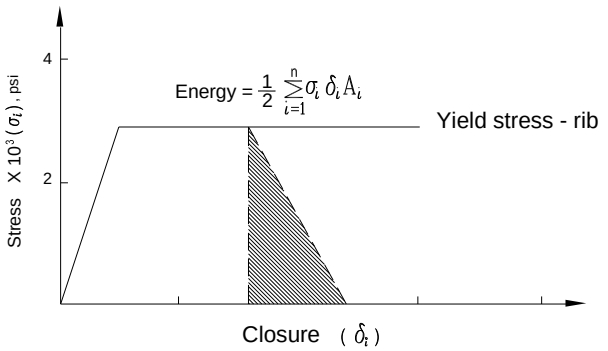

Fig. 9.3.7 Energy release model (Maleki et al., 1987)

Table 9.3.2 Critical level criteria for unstable conditions (Maleki et al., 1987)

Model	Pre-cut average stress, psi	Average cut closure, in.	Number of highly- stressed elements	Average energy released per cut, 10^3 ft-lb
Elastic-plastic	4,180	2.10	8	3,280
Strain softening	4,190	2.17	9	3,460

9.3.7 Overhanging and Arching of Thick Overlying Strata

The overhang of massive overlying strata immediately above or in close proximity to the coal is known to cause high front abutment pressure at the longwall face. Depending on the stiffness (i.e., a combination of strength and thickness) of these overlying strata, they break periodically and induce periodic weighting. Study by Haramy et al., (1987) showed that the occurrence of face bumps correlates well with the periodic breakage and weighting of the cantilevered beams, and this effect was reflected by the periodic up and down of the measured shield leg pressure.

Arching of the overlying thick strata over two panel widths and the proximity to sandstone channels caused high side abutment pressure in the Utah coal field which, in turn, caused an increase in the frequency of bumps at the tailgate corner (Agapito et al., 1997; Agapito and Goodrich, 2000). For a panel width 630-820 ft (200-250 m), there were no significant bumps in the 1st and 2nd panels. Bumps near the tailgate corner occurred in the 3rd panel when the panel had retreated for a distance of 1,509 ft (460 m) at a depth of 1,968 ft (600 m). No bumps occurred in the tailgate chain pillars.

9.4 MAGNITUDE AND DAMAGES OF COAL BUMPS

Mining-induced overburden movements, notably roof caving in the gob of longwall and pillar extraction mining have been known to generate seismic events. Mine-induced seismicity (MIS) has been a subject of study since the 1960s, especially in Utah's Wasatch Plateau and Book Cliffs coalfields. The MIS waves are different from those of naturally occurring earthquakes

(Swanson et al., 2008) due mainly to wave propagation path effects. From a ground control point of view, the most relevant information is the source location of the events. Recent study (Pankow et al., 2008) indicates that the event location can be estimated with an absolute errors of -656 ft (-200 m) or less (horizontal distance), depending on the array of seismic stations. However, using microseismic technique with a proper array of geophones over the target panels, more accurate source location is feasible (Heasley et al., 2001) (see Section 9.6.1 for detail).

There are no standards of recording the magnitude and damage of a coal bump. Three methods have been used: description of the bump scenes, bump energy of simulated bump tests in the laboratory, and seismic event.

The intensity of coal bumps ranges from minor thumping of coal pillars to large quantities of coal being suddenly ejected into the mine. Bumps have caused various degrees of damage to mine structures and equipment. Some documented examples include the following: more than 100 pillars were involved in the bumps (Descour and Miller, 1987); the ejected coal amounted to 1,500 tons (Peng, 1986); a violent bump manifested itself along a distance of 7,000 ft (2,133.6 m) (Peperakis, 1958); the shearer was pushed over the panline and against the shield; a continuous miner, a roof bolter and a shuttle car were pushed up to 70 ft (21.3 m) away. It must be emphasized, however, that bumps that resulted in fatalities and injuries were, in many cases, small, involving only a few feet of rib bursts.

In their simulated model pillar bump tests in the laboratory, Babcock and Bickel (1984) found that bump momentum and kinetic energy are 65-2,300 gm-cm/sec and 1-281 milli-joules. The momentum, *M*, and kinetic energy, *KE*, are defined as

$$M = \sum_{i=1}^{n} dm_i v_1 \tag{9.4.1}$$

$$KE = \sum_{i=1}^{n} dm_i \frac{v_i^2}{2} \tag{9.4.2}$$

where dm_i and v_i are the mass and velocity, respectively, of the i^{th} mass thrown by the burst.

Numerous reports have been cited about bumps being felt on the surface. Most bumps were small, on the order of less than 2 on the Richter scale. The largest ones recorded by seismological stations were 4.2-4.5 in central Appalachia (Iannacchione and Zelanko, 1995) and 4.2 in Utah (Arabasz et al., 2005; Heasley et al., 2001).

In monitoring the mining-induced seismicity (MIS) around the Trail Mountain area of central Utah where longwall mining was active about 2,198 ft (670 m) below surface, Arabasz et al., (2005) found that the observed seismicity was highly correlated with mining activity both in space and time. The densely clustered epicenters were laterally within 820 ft (250 m) on either side of the active longwall panel and within ± 1,968.5 ft (600 m) of the mine level. The rates of MIS correlated with mine shifts. During weekdays, when no mining was performed, the rates of MIS were about one tenth of those when regular mining was conducted. The magnitude ranged from less than zero to 2.2 on the Richter scale, mostly 0.4-1.2, with an average of 0.8. The ground-motion induced by coal bumps can be predicted by the following equations (McGarr and Fletcher, 2005)

$$Log\ v = -3.214 + 0.961M - 1.46\ log\ R - 0.403R + 0.337 \tag{9.4.3}$$

$$Log\ a = -0.9892 + 0.8824M - 1.355\ log\ R - 0.1363R + 0.337 \tag{9.4.4}$$

where v and a are particle velocity (cm/sec) and acceleration (cm/sec^2), respectively, M is moment magnitude or Richter scale, and R is epicenter distance.

9.5 METHODS OF BUMP CONTROL

Two methods are available for bump control. The most desirable and long-lasting one is through proper mine design and planning (Campoli and Heasley, 1989), while the other is to perform de-stressing program incorporated into the mining cycle. The former is mine or panel layout and the latter includes stress monitoring by drilling yield tests, volley firing, and water infusion.

9.5.1 Mine Layout and Cutting Sequence

According to Iannacchione and Zelanko (1995), 67% of the bumps were caused by the act of cutting and 22% by coal loading. 22% of them took place in non production shifts. Accordingly, mine layout and cutting sequence are critical factors in controlling bumps.

1. Room and Pillar Mining

Methods for bump prevention include: (1) The pillar line must be straight and involves no pillar line points, i.e., no individual part or parts sticking out of line into the gob. If these exist, the pillar line should be sub parallel to natural fracture systems for convenience of gob caving. Development should be done outby the abutment zone (Holland, 1958b). Do not split pillars on or near the extraction line. Conversely, Varley (1986) encouraged recovering pillars between the gob and abutment zone by splitting the last row of pillars in a long pillar line such that the stumps yield. (2) Employ an open-end method of pillar extraction. Cutting should be directly away from, not toward, the pillar line (Peng, 2007). (3) Extract as much coal as possible, leaving no remnant pillars in the gob (Holland, 1958b; Campoli et al., 1987). (4) Roof span overhanging the gob should be as small as possible (Campoli et al., 1987).

Talman and Schroder (1958) found that pillars less than 46 ft (14 m) or larger than 161 ft (49 m) almost never bumped, and they developed a thin-pillar mining method for barrier splitting. In this method, mining geometry and the cutting sequence are such that only pillar blocks less than 46 ft (14 m) and larger than 161 ft (49 m) were used (Holland and Thomas, 1954). Entries and crosscuts are 20 ft (6.1 m) wide. Fig. 9.5.1 shows the cutting sequence (Iannacchione and Zelanko, 1995).

A mining technique practiced successfully in a southern West Virginia coal mine in the 1970s and 1980s for bump control was extensively studied by the then U.S. Bureau of Mines (Campoli et al; 1989; Haramy et al, 1985; Oyler et al., 1987). It consisted of an ordered cutting sequence in a group of three pillars in the first 3-4 rows of pillars outby the pillar line such that the abutment pressure is directed gradually away from the pillar line (Fig. 9.5.2). Chain pillars were 60 ft wide by 70 ft long (18.3 x 21.3 m). First, a bump cut of 20 x 20 ft (6.1 x 6.1 m) was made on the gob side of the 3rd row of pillars. Second, center splitting was completed in the 2nd row of pillars, and finally wing cuts were made to extract the stumps in all three pillars of the first row. Campoli et al., (1989) instrumented the retreating panels and found that the technique transferred the abutment pressure up to 8 rows away from the pillar line, greatly and effectively minimizing bump potential. Zipf and Heasley (1990) also found that this technique is superior to the traditional pillar extraction techniques, such as single split-and-fender, pocket-and-wing, and open ending in reducing bump potential.

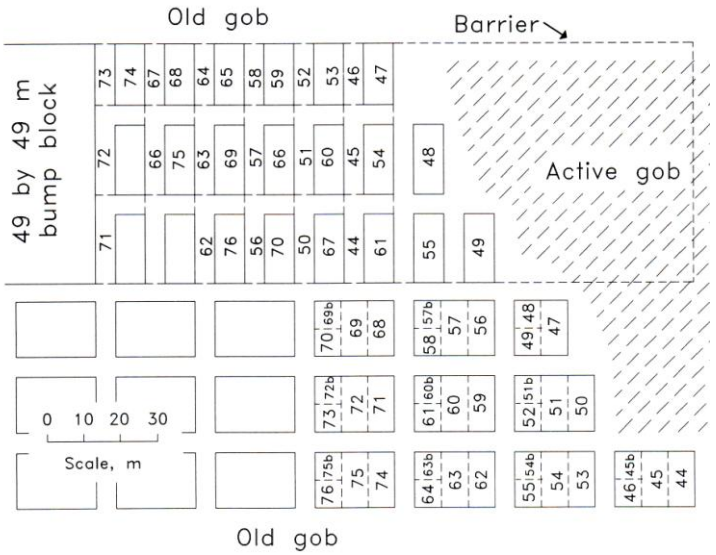

Fig. 9.5.1 Thin pillar mining method (Iannacchione and Zelanko, 1995)

For pillar extraction, Holland and Thomas (1954) recommended the open-end method for bump control. Extraction should be well-planned so that no pillar line point or points are formed along a pillar line or converging pillar lines. Pillar line should be oriented parallel to the natural fracture system of the roof. No stump pillars are left in the gob (Holland, 1955). In Figure 9.5.3, several preferable open-end pillar mining methods are illustrated.

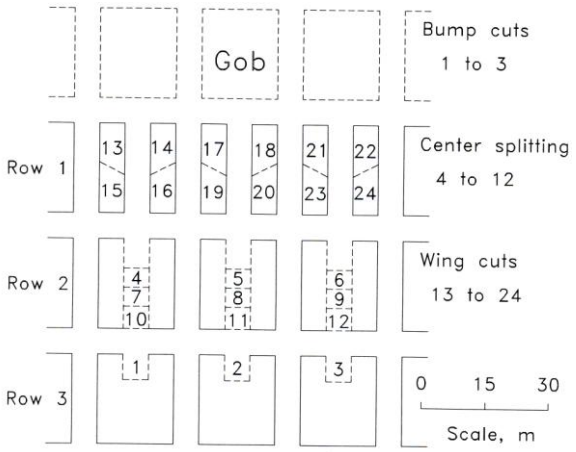

Fig. 9.5.2 Three-stage pillar recovery method (Iannacchione and Zelanko, 1995)

2. Longwall Mining

Due to its rigid structure in panel layout and the chain pillars' susceptibility to bumps, bump control for longwall mining emphasizes the gateroad system design. Two gateroad system designs have been demonstrated successfully for bump control: two-entry yield pillar and four-entry yield-abutment-yield pillar systems.

A. Two-entry yield pillar system

(1) History of yield pillar design

The two-entry system has been practiced only in coal mines in Utah. In the early 1960s, coal mines in central Utah, where cover is more than 1,000-1,500 ft (304.8-457.2 m) deep, employed the room-and-pillar mining method with conventional pillar sizes of 40 x 80 ft (12.2 x 24.4 m), 60 x 60 ft (18.3 x 18.3 m), and 60 x 80 ft (18.3 x 24.4 m). They were subjected to bumps, often severe (Agapito et al., 1988; DeMarco et al., 1993; Kripakov and Kneisley, 1992). Longwall mining was then introduced with three- and two-entry systems. Chain pillars with greater than 40 ft (12.2 m) width, including 40 x 80 ft (12.2 x 24.4 m), 45 x 80 ft (12.2 x 24.4 m), 50 x 50 ft (15.2 x 15.2 m), and 60 x 80 ft (18.3 x 24.4 m) were initially used. Bumps and roof falls occurred in all chain pillar systems, regardless of whether the mine was two- or three-entry system. In comparison, everything being equal, the three-entry system has 36 % more exposed roof area, 33 % more intersections, and twice as many number of pillars and total pillar width as the two-entry system, leading to a higher potential for ground control and bump problems. Consequently, the two-entry system was adopted and several pillar sizes were experimented with.

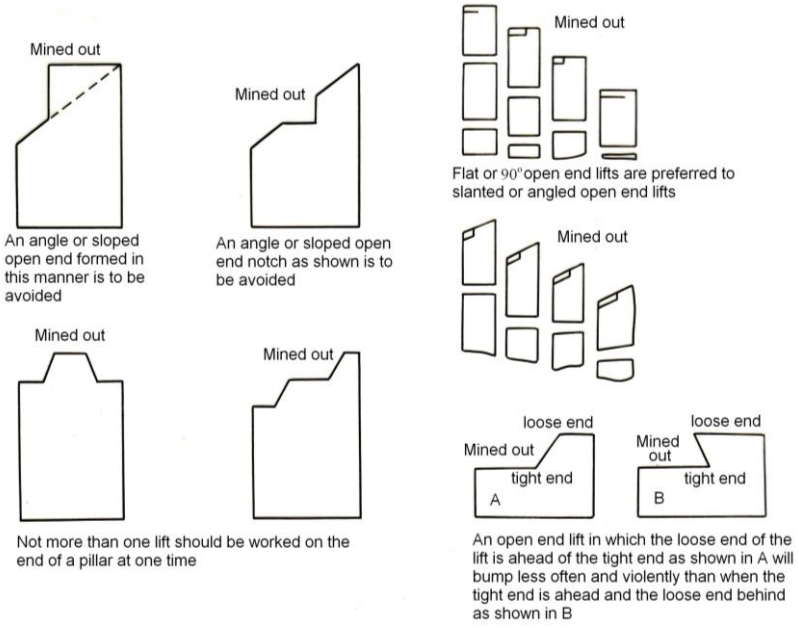

Fig. 9.5.3 Recommendations for open-ended pillar extraction methods (Holland and Thomas, 1954)

In the two-entry system, 40 ft (12.2 m) and 50 ft (15.2 m) yield pillars under high cover were liable to bumps and resulted in roof and floor problems. Comparison between 30 ft (9.1 m) and 40 ft (12.2 m) yield pillars showed that a 30 ft (9.1 m) pillar seldom bumped while the 40 ft (12.2 m) pillars bumped more frequently and in larger magnitude (Koehler, 1994).

For cover depth greater than 1,500 ft (457.2 m), the 20-30 ft (6.1-9.1 m) pillars in 6-10 ft (1.8-3 m) mining height would yield either after development or when the first longwall face approached, with the 30 ft (9.1 m) pillars yielding mostly after the first longwall face had passed. The 30 ft (9.1 m) yield pillars have been successfully used since the 1960s.

For the four-entry 30-120-30 ft gateroad system under 1,300-1,500 ft (396-457 m) cover, ground pressure and entry closure measurements confirmed that the 30 ft (9.1 m) wide yield pillar was partially shielded from the first panel loads by the 120 ft (36.6 m) abutment pillar, and consequently, experienced only minor yield until the approach of the second panel face. Complete yield of the 30 ft (9.1 m) yield pillar occurred when the second panel was approximately 20 ft (6.1 m) inby the instrumentation site (Koehler et al., 1996). However, the very high pressures sustained in the pillars led to the conclusion that theses pillars may bump when the cover exceeds 1,300-1,500 ft (396-457 m).

Maleki et al., (2003b) monitored pillar pressure and rib dilation in the Rock Canyon seam for the three- and two-entry 30 ft (9.1 m) yield pillar gateroad systems. They found that yielding of yield pillars in the three-entry system resulted in a significant load transfer toward the solid panel, which was detrimental for secondary use of these gateroads as tailgate because it promoted longer cantilevers supported by residual strength of gate pillars. They also found that yielding of yield pillars occurred closer to the face under the influence of high cover and the effectiveness of yield pillars in limiting strain energy accumulation while controlling roof-floor convergence outby the face position.

Under strong roof and immediate floor (UCS = 9,000-24,000 psi or 62.1-165.5 MPa) and soft coal (UCS = 600-1,000 psi or 4.1-7.6 MPa) conditions, a 30 ft (9.1 m) pillar would bump before yielding. Bumps ceased, but the frequency of audible bumps increased when pillars were reduced to 20 ft (6.1 m), indicating a more rapid yielding of pillars (Varley, 1986).

The 20 ft (6.1 m) pillars were the minimum feasible width, considering the requirements for power center storage, face development equipment manipulation, place-change mining scheduling, parking space, etc. In one multiple-seam case, the 18 x 80 ft (5.5 x 24.4 m) pillars were found to be successful (DeMarco et al., 1993), because they reduced seam interaction. A three-entry system with two-row of yield pillars had been successful in one case under 700 ft (213.4 m) of cover.

Yield pillars of 30 ft (9.1 m) were not successful under very strong roof and floor conditions. However, a trial of 15-20 ft (4.6-6.1 m) pillars using room and pillar with pillar extraction produced no ground control problems. This apparent difference in pillar behavior prompted DeMarco et al., (1993) and Kripakov and Kneisley (1992) to propose that the high degree of confinement under strong roof and floor conditions enhanced the 30 ft (9.1 m) pillars to become non-yielding and may require yield pillars in the 15-20 ft (4.6-6.1 m) range.

Experience also indicates that the two-entry yield pillar system will only work when the roof and floor are competent, and yet not too strong; that stiff and yet yielding supplemental supports are required to keep the tailgate open when the second panel is being mined; and that in practice, the window of yield pillar design is restricted to 28-32 ft (8.5-9.8 m) range (Peng, 2007).

Unfortunately, the success of the two-entry yield pillar system in alleviating pillar bumps does not apply to the longwall face area. In fact, face bumps seem to be getting worse as shown by recent fatality records. It is very likely that tailgate yield pillars have transferred the side abutment pressure from the previous panel to the solid coal block, causing bumps at the tailgate corner of the subsequent panel.

(2) Design of yield pillars to prevent bumps

Morsy (2003) and Morsy and Peng (2003) proposed a yield pillar design methodology for bump-prone longwall mines (see Section 5.4.2 on p. 264 for details). The stability of a yield pillar is defined by three parameters: core stability factor (CSF), pillar bump index (PBI), and

rib zone ratio (RZR). The CSF provides a measure of stress inside the pillar core with respect to its yielding stress. The PBI is a measure for the storage and dissipation of elastic strain energy and plastic dissipated energy, respectively. The RZR is a measure of the percentage of pillar rib that has the post-failure slope greater than the local mine stiffness.

The RZR is inversely proportional to the maximum shear limit, indicating the rib of the pillar has a higher tendency to bump with smaller shear limits because the rib is brittle under small shear limits. The PBI is directly proportional to the maximum shear limit, meaning the pillar could bump with higher shear limits. This behavior can be explained by the ability of the pillar to store more elastic strain energy when it gains more confinement by increasing the maximum shear limit. The CSF is inversely proportional to the maximum shear limit. The yield pillar has a lower chance of yielding when the CSF is close to one. In that case, the elastic core vanishes. This condition could be achieved under a lower shear limit.

B. Four-entry combination of yield and abutment pillar system

In central Appalachia where the cover is more than 2,000 ft (609.6 m), longwall mining employing the four-entry abutment-yield-yield pillar system was originally used in the 1970s (Campoli et al., 1987; Iannacchione and Zelanko, 1995). The abutment pillars were 100 x 100 ft (30.5 x 30.5 m). During the second panel mining, the side abutment of the mined first panel and the front abutment of the second panel overlapped and produced high stress concentration at the tailgate T-junction area. The abutment pillars adjacent to the tailgate bumped frequently and severely (Fig. 9.5.4A). It was then changed to a four-entry yield-abutment-yield system (Fig. 9.5.4B). The smaller pillars on both sides of the abutment pillars located at the center would yield and prevent floor heave as experienced with the previous abutment-yield-yield system. The central abutment pillars offer support to the roof. When and if bumps occur, the working face is shielded with a row of yield pillars, ensuring the safety of miners and equipment at the face (see also Fig. 7.2.2 on p. 318).

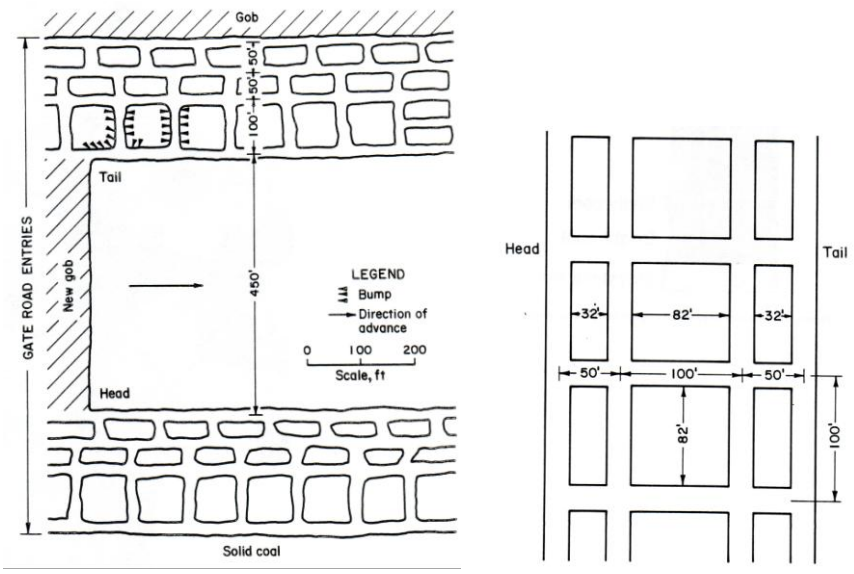

A **B**

Fig. 9.5.4 Four-entry gateroad systems: A, abutment pillar next to tailgate B, abutment pillars at the center

Later the yield-abutment-yield system was employed (Campoli et al., 1990); initially, 30 x 80 ft (9.1 x 24.4 m), 80 x 80 ft (24.4 x 24.4 m), 30 x 80 ft (9.1 x 24.4 m), and later 20 x 80 ft (6.1 m), 120 x 180 ft (36.6 x 54.9 m), and 20 x 80 ft (6.1 x 24.4 m). The abutment pillars bumped in both systems at different periods of mining: Both abutment pillars did not bump under headgate loading. The 80 x 80 ft (24.4 x 24.4 m) pillars experienced structural failure when they were 1,000 ft (304.8 m) and began to bump 500 ft (152.4 m) outby the face. These abutment pillars failed violently, resulting in load transfer to the panel being mined and bumping at the tailgate corners.

The 120 x 180 ft (36.6 x 54.9 m) pillars, however, experienced structural failure when they were 200 ft (61 m) outby and began to bumps 100 ft (30.5 m) inby the face. Bump intensity was greatly reduced with the larger abutment pillars and effectively shielded bumps at the tailgate corners.

9.5.2 Stress Monitoring by Drilling Yield Tests

Figure 9.5.5 shows the bump control program sequence using the drilling yield test method. High stress or abutment zones at the longwall face and pillar ribs are located by drilling yield tests. If they are outside the critical zone, coal mining continues. If they are within the critical zone, de-stressing through blasting or water infusion is performed to release the stress. This way, coal bumps at the face and pillar ribs are alleviated.

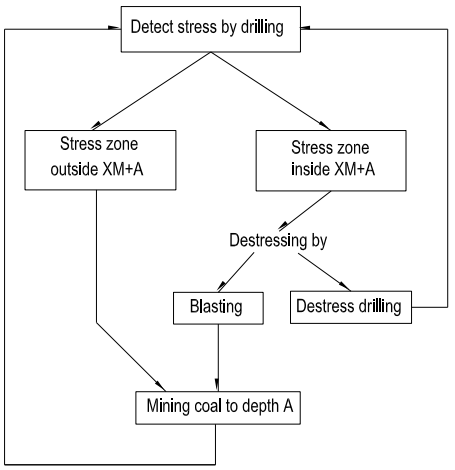

Fig. 9.5.5 Drilling yield stress monitoring program (modified from Varley, 1986)

By the drilling yield testing technique (Neyman et al., 1972; Brauner, 1994), a hole 2-3 in. (50.8-76.2 mm) in diameter is drilled in the coal seam ahead of a working face. As drilling proceeds from the rib toward the center of the coal blocks, the quantity of cuttings ejected and any dynamic effects such as audible knocking, grating, and jamming of the drill in the hole are observed. Highly stressed zones are characterized by increased activity, and thus zones of decreased or increased pressures can be determined. The closer to the ribside, the greater is the danger of a bump. Figure 9.5.6 shows typical curves of drilling progress in a seam where a coal bump is likely (Fig. 9.5.6A) and unlikely (Fig. 9.5.6B). Observation in Polish coal mines (Neyman et al., 1972) indicated that a safe state exists when the highly stressed zone is located a distance greater than 3.4 H from the ribside, where H is seam thickness. A dangerous state

exists when this zone is located between 1.5 H and 3.4 H, and a critical state exists when it is located less than 1.5 H from the ribside

The drilling yield technique is also being practiced in Germany's Ruhr coal field (Brauner, 1994). The 2 in. (50.8 mm) diameter holes are drilled from the face and ribs at various intervals, being 30 ft (9.1 m) near the longwall face ends and 120 ft (36.6 m) near the center of the face. The nearest point to a highly stressed zone by testing drilling is identified by:

(1) Cuttings, 8 liters or more per meter of advance accompanied by a coal bump.
(2) A hard bump, one that can be heard 100 meters away at any time.
(3) Cuttings, 15 liters or more per meter of advance with no accompanying noise from the coal, which indicates that caution must be exercised in drilling the hole further.

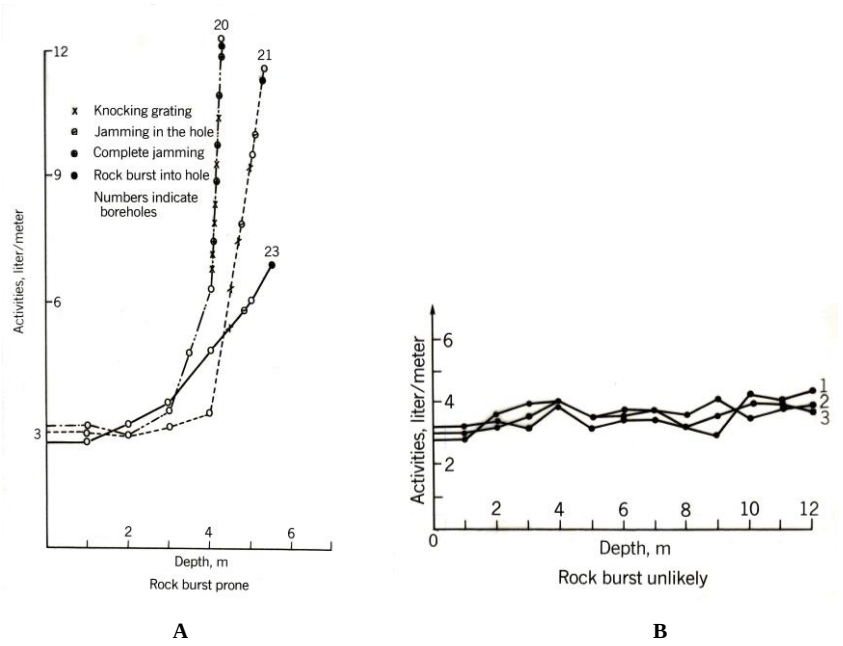

Fig. 9.5.6 Drilling yield tests, bumps are A, likely, B, unlikely (Neyman et al., 1972)

If the highly stressed zone is located at a distance of 3H+A or more, the face is safe to advance for a distance of A, where H = mining height and A is the scheduled distance of face advance during a certain period of time before the next drilling (e.g., a shift). However, if the highly stressed zone is located at a distance less than 3H + A, the holes must be de-stressed by volley firing.

The relationship between applied stress and cuttings can be estimated by (Haramy and McDonnell, 1988b)

$$\sigma_v = 123 \log\left(\frac{V_c}{V_e}\right) + 18 \tag{9.5.1}$$

where σ_v is applied vertical stress, MPa, V_c is volume of cuttings, and V_e is nominal hole volume.

The drilling yield test was once used in a bump-prone coal mine in Colorado in the 1980s (Varley, 1986). Two-inch (50.8 mm) diameter holes were used to minimize triggering severe bumps. As the holes were drilled, cuttings per meter, occurrence of bumps, gas pressure, squeezing on drill steel, and the depth of these observations were recorded. The location of zones of abutment could be determined from the data collected. The critical zones that would pose hazards to miners are:

(1) 15 liters of cuttings per meter of hole, or
(2) 8 liters of cuttings per meter accompanied by a bump, or
(3) Hard bump triggered by drilling (audible at a distance of 328 ft or 100 m or more away).

The volume of cuttings produced per meter with no pressure is about 2 liters. Harder coals produce fewer cuttings than softer ones.

As the pressure on the coal increases and compresses the hole, it causes the auger with a fixed diameter to cut more coal, producing more cuttings. As the drill enters the abutment zone, the rapid pressure increase will catch the auger flights, drawing the drill steel into the deep end of the hole. This drawing steel into coal usually represents the precursor of a bump triggered by drilling (Fig. 9.5.7).

Holes were drilled on 100 ft (30.5 m) centers along the face to a depth of 43 ft (13.1 m). If critical stress was located less than 40 ft (12.2 m) from the face, de-stressing was required. An average of 9 holes was drilled each cycle requiring 9 man hours.

The criteria for determining the location of the highly stressed zone is xH + A, where x = 3 for the faces and 2 for ribs and pillars.

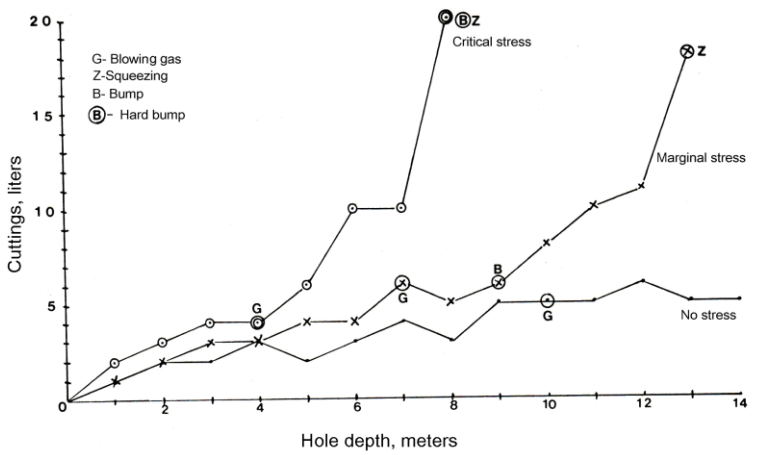

Fig. 9.5.7 Stress detection drilling (Varley, 1986)

9.5.3 De-Stressing

Once the abutment or high stress zones are found, they must be de-stressed in order to safely mine those areas. De-stressing destroys the structural integrity of the coal so that it cannot store enough energy to fail violently. Several methods are available for de-stressing, including drilling and blasting, water infusion, and drilling through large diameter holes.

It must be emphasized that de-stressing requires miners' presence at or close to the sites where potential bumps exist. Therefore, safety measures must be developed in advance and strictly followed.

1. Drilling and Blasting

Blasting reduces the stresses in coal through two effects (Brauner, 1994): fracturing reduces coal strength around the hole and vibration reduces the friction between coal and adjacent rocks, including partings.

The number and spacing of the shotholes are based on the drilling test results. The blastholes are normally the drilling test holes that indicate high stress zones, i.e., their depth depends on the location of high stress zones. However, face areas are shot to a distance not less than the planned advance before repeating the drilling yield test again. Only permissible explosives are used. The amount of explosive charges used is designed such that a contained explosion occurs, i.e., they do not throw any burden. Otherwise a new free coal face could be more bump-prone than the old one.

After detonating the charges, holes are drilled to check the blasting results. If de-stressing does not achieve the desired effect, check holes are charged and fired again.

2. Water Infusion

Brauner (1994) showed that the strength and elasticity of coal decreases with increasing moisture: on average, increasing moisture content from 1 to 5 %, the UCS of coal is reduced by 30-40 % and elastic modulus by 30-60 %. Figure 9.5.8 shows a comparison of the stress-strain curves of the same coal under dry and saturated conditions. It is quite obvious that strength, elastic modulus, and bump energy index are greatly reduced with saturated coal. In fact, saturation makes the coal not liable to bump.

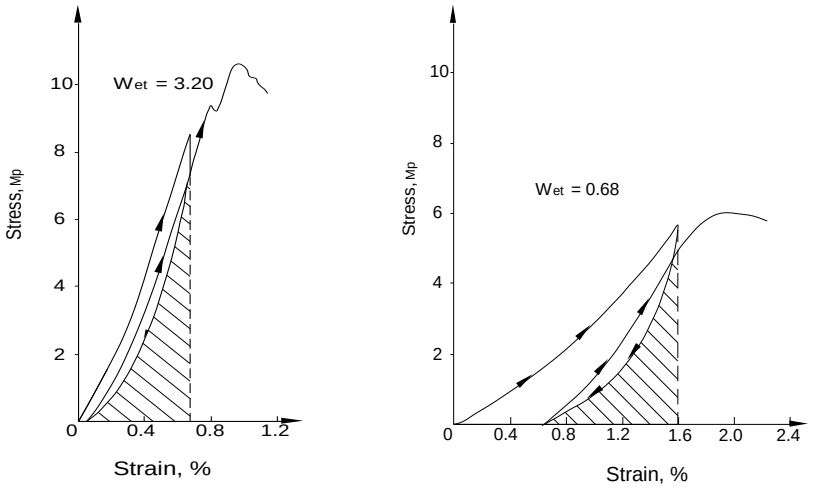

Fig. 9.5.8 Stress-strain curves of dry and saturated coal (Brauner, 1994)

Water infusion is used for respirable dust suppression, and hydraulic fracturing is commonly used to enhance methane drainage in U.S. longwall coal mines (Peng, 2006). High pressure water has been used to fracture coal for bump control (Varley, 1986).

Holes 100 ft (30.5 m) long on approximately 75 ft (22.9 m) centers are drilled on the tailgate. Immediately after drilling, a hydraulic hose is inserted into the hole and allowed to be compressed and seized by the surrounding coal. Water pressure inside the hose is then increased to 4,000 psi (27.6 MPa). Within 20 minutes or so, audible noises are heard indicating hole fracturing. At this time, water is pumped continuously at a rate of 10-30 gpm (gallons per minute) (45.5-136.4 liters/min) to maintain the hole pressure around 4,000 psi (27.6 MPa). Water infusion discontinues when the pumping rate exceeds 100 gpm (454.6 liters/min) which normally take 3-20 days. In the water infusion areas, the frequency of occurrence of critical stress zones was reduced to zero from 7 per 100 ft (30.5 m) for areas without water infusion (Varley, 1986). Longwall shield hydraulic fluid has also been used to prevent bumps of gateroad chain pillars (Buchsbaum, 2006).

It must be emphasized that while some bumps are preceded by rapid increases in the microseismic noise rate, others show no rate increase, and sometimes while rapid rate increases are measured, no bumps occur (Blake et al., 1974; Blake, 1982). Analysis of microseismic activities generated at the face and tailgate of a deep advancing longwall in Colorado showed that while overall microseismic events may increase immediately prior to or during a bump, the actual bump area either quieted down or never indicated microseismic activity (Kneisley, 1989). Figure 9.5.9 clearly shows that microseismic events, attributable to a combination of mining- and de-stressing-induced fracturing, occurred around the panel center toward the headgate side, but did not occur at the area of bumps located near the headgate. It appears that fracturing and energy release in the area of increasing microseismic activity transfer the load to the non-failed portion of the face. This non-failed area, loaded by a combination of the front abutment pressure, side abutment pressure from the previous panel, and the transferred load from the adjacent fractured zone at the face, released its energy violently when it was mined into. This case study pointed out an important point, in that de-stressing must be carefully planned so that the areas to which the load is transferred do not overload and bump.

9.6 PREDICTION OF BUMPS BY THE MICROSEISMIC METHOD

9.6.1 Microseismic Detection

It has been demonstrated that rock fracture processes under compression consist of three distinct stages: crack initiation, propagation, and ultimate fracture, and that it is the coalescence of numerous cracks rather than the propagation of a single crack that leads to ultimate failure (Peng and Ortiz, 1972). Each stage of crack development generates a stress wave that radiates and propagates away. This stress wave is called rock noise or **acoustic emission**, the magnitude of which is proportional to the size of the crack and the amount of displacement. The frequency spectrum of rock noise is very broad and ranges from 50 to more than 100,000 cycles per second (Hz). Hardy (1975) found that the frequency spectrum for the rock noise associated with underground longwall coal mining is between 160 and 500 Hz with a predominant frequency spectrum at 320 Hz. Both P (compression) and S (shear) waves are present in rock noise and most energy is associated with the shear wave. As a wave travels, its magnitude decreases with distance. This is **attenuation**. Attenuation is proportional to wave frequency, the higher the frequency, the greater the attenuation.

When rock is subjected to uniaxial compression, practically no noise is found at the initial load. As the load increases, rock noises are generated and gradually increase in number. When failure is approached, the rock-noise count increases very rapidly (Fig. 9.6.1). These

phenomena of rock-noise developments have also been verified in the field (Fig. 9.6.1B). Since each rock noise is associated with each stage of crack development, an increasing number of rock noises correspond to an intensive crack development, which in turn indicates its stage of approaching impending failure. Consequently, a sharp increased rate of noise count can be used as a warning of impending failure.

The technique of using rock noise to predict impending failure involves the detection of rock noises, the determination of sources from which the detected rock noises are generated, and interpretation of rock-noise data (Blake et al., 1974).

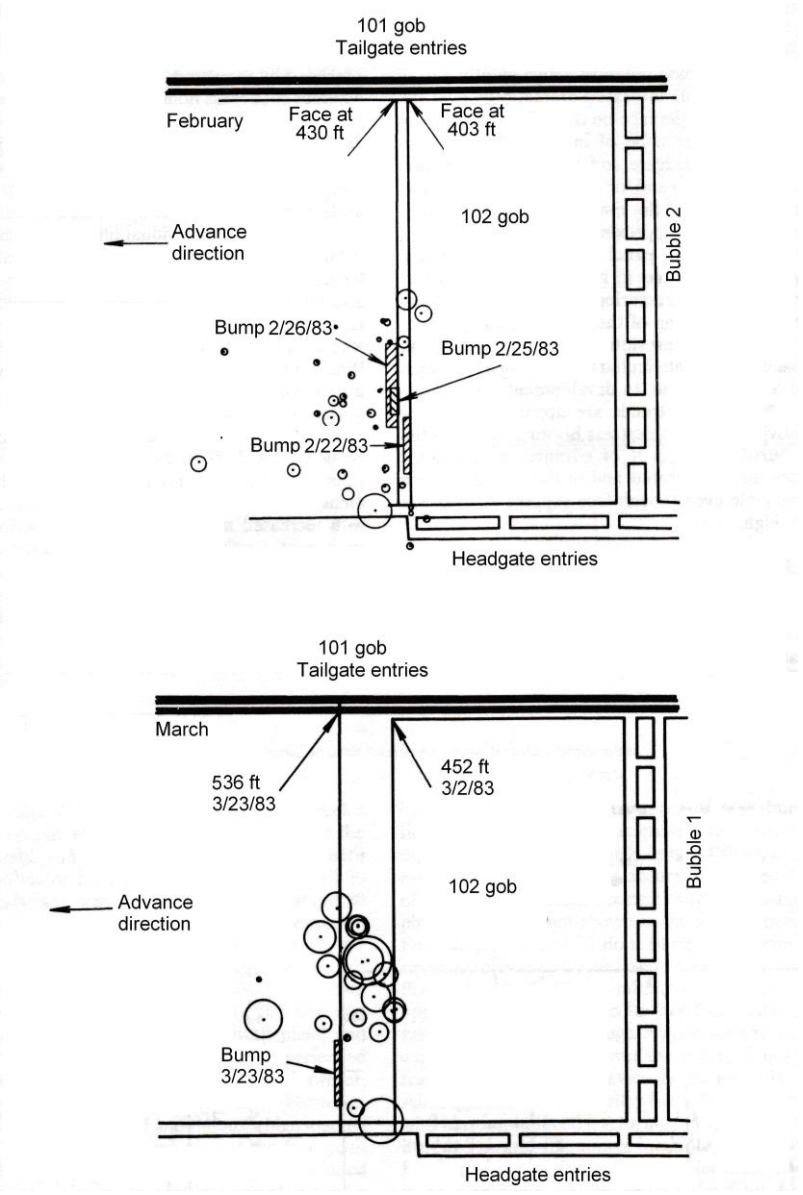

Fig. 9.5.9 Microseismic source and face bump location (Kneisley, 1989)

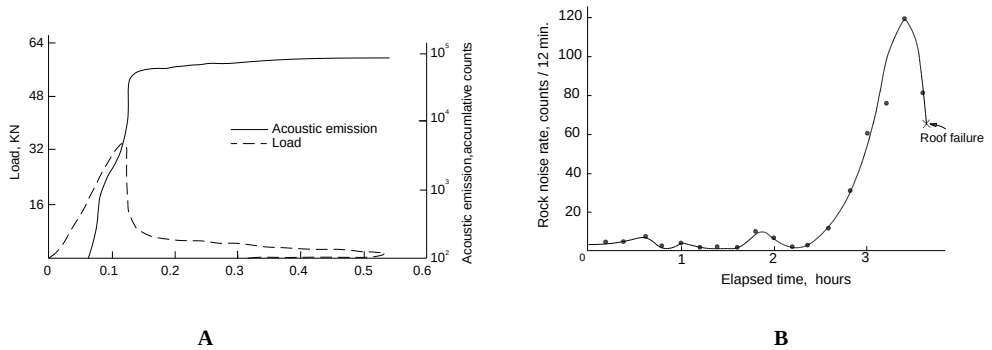

Fig. 9.6.1 Rock-noise development and impending roof fall A, laboratory specimen, B, underground entry roof (Courtesy U.S. Bureau of Mines)

9.6.2 Detection of Rock Noise

Geophones are used to detect a rock noise as it passes through the rock and convert it to an equivalent electrical signal, which is then amplified for permanent recording. The passage of a rock-noise can be detected by measuring particle displacement, velocity, or acceleration. A particle displacement gage is most sensitive for low-frequency vibration, a velocity gage for medium frequencies, and an accelerometer for high frequencies. Since the rock-noise frequency spectrum is very broad, a velocity gage or accelerometers are most commonly used. The gage selected should have a wide, flat range response so that it can respond equally well to a wide frequency range. Velocity gages can be mounted on plastic blocks cemented to the roof or floor, whereas accelerometers can be mounted on the roof or in a hole. Generally, at least four gages are used for a good source location. They should be located around the area of suspected instability and positioned in a three-dimensional array. The coordinate of each geophone is then determined to the nearest 1 ft (0.3 m) for source location calculation.

9.6.3 Rock-Noise Source Location

To locate the source of a rock-noise, the velocity at which a noise wave travels must be known first. This can be determined by detonating a small explosive and noting the arrival time of each wave train at each geophone. The seismic velocity can then be determined as follows:

$$V_{pi} = \frac{D_i}{T_i} \tag{9.6.1}$$

$$V_{si} = \frac{D_i}{S_i} \tag{9.6.2}$$

where the subscript i denotes parameters for the i^{th} geophone, V_p and V_s are the velocities of P- and S-waves, respectively, D is the distance between the geophone and the explosive detonating position, and T and S are travel times of P- and S-waves, respectively, from the blast to the geophones.

Microseismic source location techniques involve the determination of the coordinates of the unknown sources using wave arrival time and the geometrical relationship of the

positioned geophone based on a P-wave or S-P-wave method (Blake et al., 1974). The distance between the source and the i^{th} geophone is

$$d_i = V_i^p T_i^p \tag{9.6.3}$$

$$d_i = \frac{\Delta T_i^{s-p}}{(1/V_i^s) - (1/V_i^p)} \tag{9.6.4}$$

Where V_i^p and V_i^s are the P- and S-wave velocities from the source to the i^{th} geophone, respectively, T_i^p and T_i^{s-p} are the P-wave arrival time and the difference in arrival times between S- and P-waves at the i^{th} geophone, respectively.

The ultimate objective is to determine the source coordinates via the distance d_i such that

$$d_i = \sqrt{(x-a_1)^2 + (y-b_1)^2 + (z-c_1)^2} \tag{9.6.5}$$

where x, y, z and a_1, b_1, c_1 are the coordinates of the unknown sources and the i^{th} geophone, respectively.

However, in an actual microseismic monitoring application, the true arrival time of a P-wave can not be directly measured because the source is unknown. Therefore, the arrival time of the P-wave at the i^{th} geophone is generally measured from the closest or 0^{th} geophone. The true distance between the i^{th} geophone and the source is then the summation of distances from the i^{th} to the 0^{th} geophone, d_i, and from 0^{th} geophone to the source, d_o:

$$d_i + d_o = \sqrt{(x-a_1)^2 + (y-b_1)^2 + (z-c_1)^2} \tag{9.6.6}$$

Substituting Equation 9.6.1 for d_i gives

$$V_i^p T_i^p + \sqrt{(x-a_o)^2 + (y-b_o)^2 + (z-c_o)^2} = \sqrt{(x-a_1)^2 + (y-b_1)^2 + (z-c_1)^2} \tag{9.6.7}$$

where a_o, b_o and c_o are the coordinates of the 0^{th} or closest geophone and i assumes values from 1 to 4.

From the S-P-wave method, simply equate Equation 9.6.4 to Equation 9.6.5 to determine the source coordinates, which yields

$$\frac{\Delta T_i^{S-P}}{(1/V_i^S) - (1/V_i^P)} = \sqrt{(x-a_1)^2 + (y-b_1)^2 + (z-c_1)^2} \tag{9.6.8}$$

where i also takes values from 1 to 4.

In solving for the source coordinates, both Equations 9.3.7 and 9.3.8 are squared for simplification, but in order to eliminate the radical term in the P-wave method and the squared coordinates term in the S-P-wave method, it is necessary to subtract equations for i = 2, 3, and 4 from i = 1 for both methods. The result is then three linearly independent equations for three unknowns. Therefore, for the S-P wave method, at least four geophones are required, whereas

five is the minimum for the P-wave method because each equation is made up of information from two geophones.

However, rock-noise sources are frequently located beyond the geophone array. Inaccuracy in the aforementioned methods increases as the source moves away from the array. This disadvantage can be corrected by using the least-squares method (Blake et al., 1974), which considers information from more than the minimum number of geophones required, i.e., four for the S-P-wave method and five for the P-wave method. It has been reported that one more geophone than the minimum number required can increase the accuracy of source location by as much as 50 %. Table 9.6.1 shows the source location accuracies for various location methods.

Table 9.6.1 Source location accuracies (Blake et al., 1974)

Method	Distance, ft
S-P-wave	
Source inside geophone array	±10
Source outside geophone array	±15-20
Source outside array- least square	±10
P-wave	
Source inside geophone array	±10
Source outside geophone array	Not reliable
Source outside array - least square	±15-20

9.6.4 Methods of Bump Prediction

If the rock-noise sources are monitored daily in areas suspected of being unstable, the coordinates of the rock-noise sources can be plotted on a mine map for bump prediction. Contour lines of equal numbers of sources are drawn daily on the map. High contour density indicates highly stressed zones that should be monitored closely for imminent bumps. An example of utilizing this technique was the U.S. Bureau of Mines' experiment performed at the Dutch Creek #1 coal mine near Carbondale, Colorado (Figs. 9.6.2 and 9.6.3) (Leighton and Steblay, 1975). The bump area began to release noise on April 3 (Fig. 9.6.2a) four weeks before failure. The source of the rock noises remained fixed, but the rock noise density increased steadily as the mining operation proceeded. A bump occurred on April 30, four weeks after the first rock noise was detected in the area. It must be noted that a sharp increase in rock noise began on April 24 one week before failure, and that there was an apparent sharp decrease in noise activity preceding failure (Fig. 9.6.3).

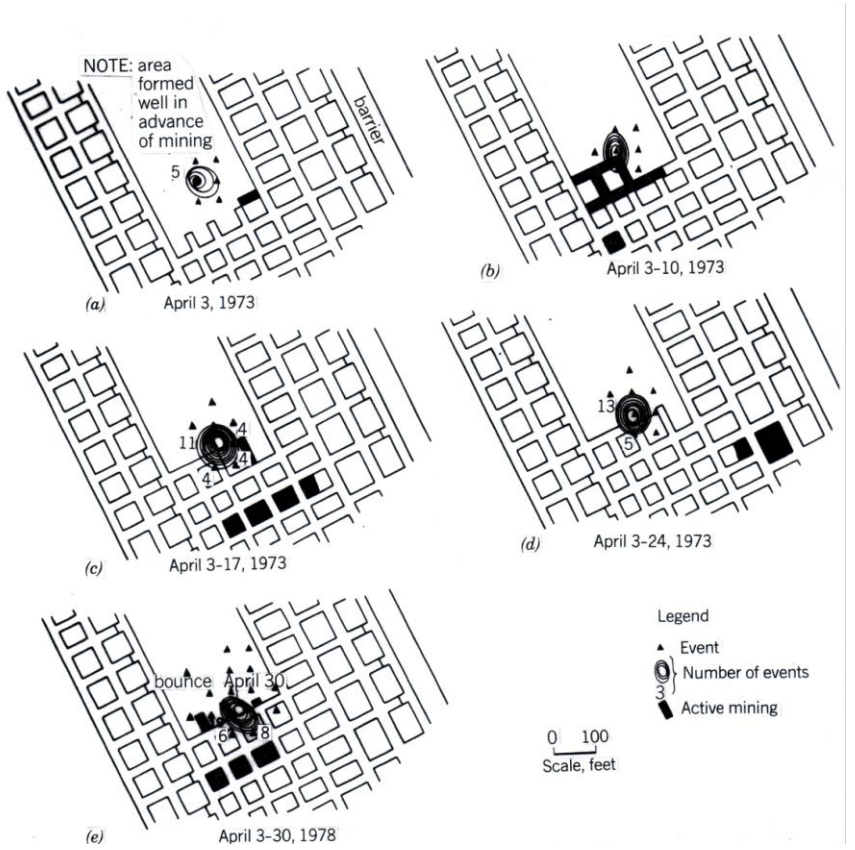

Fig. 9.6.2 Cumulative source location plots showing growth of bumps (courtesy U.S. Bureau of Mines)

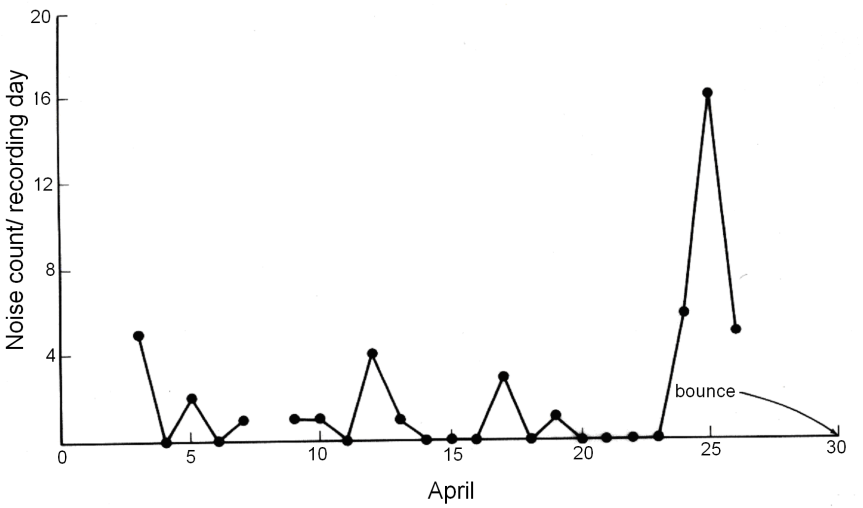

Fig. 9.6.3 Development of noise rate associated with the bumps shown in Fig. 9.6.2 (courtesy U.S. Bureau of Mines)